

## Simulation of the adsorption of simple gases on transition metals (Review)

N. V. Petrova, I. N. Yakovkin, and Yu. G. Ptushinski

Citation: *Low Temperature Physics* **31**, 224 (2005); doi: 10.1063/1.1884424

View online: <http://dx.doi.org/10.1063/1.1884424>

View Table of Contents: <http://scitation.aip.org/content/aip/journal/ltp/31/3?ver=pdfcov>

Published by the [AIP Publishing](#)

---

### Articles you may be interested in

[Spatio-temporal pattern formation during CO oxidation on Pt\(100\) at low and intermediate pressures: A comparative study](#)

*Chaos* **12**, 164 (2002); 10.1063/1.1446422

[General trends in CO dissociation on transition metal surfaces](#)

*J. Chem. Phys.* **114**, 8244 (2001); 10.1063/1.1372512

[CO oxidation on Pt\(111\)—Scanning tunneling microscopy experiments and Monte Carlo simulations](#)

*J. Chem. Phys.* **114**, 6382 (2001); 10.1063/1.1343836

[Monte Carlo simulations of a simple model for the electrocatalytic CO oxidation on platinum](#)

*J. Chem. Phys.* **109**, 6051 (1998); 10.1063/1.477230

[Calorimetric heats for CO and oxygen adsorption and for the catalytic CO oxidation reaction on Pt{111}](#)

*J. Chem. Phys.* **106**, 392 (1997); 10.1063/1.473203

---

The advertisement features a blue banner at the top with the text 'MATERIAL SCIENCE RESEARCH AT 3K – MADE SIMPLE' in white. Below the banner, there are images of various scientific instruments, including a large cryostat and a smaller optical cryostat. The Montana Instruments logo is prominently displayed in the center, with the tagline 'COLD SCIENCE MADE SIMPLE' underneath it. At the bottom, the text 'CLOSED CYCLE OPTICAL CRYOSTATS' is written in blue. The background is a light blue gradient with a subtle grid pattern.

## Simulation of the adsorption of simple gases on transition metals (Review)

N. V. Petrova, I. N. Yakovkin,\* and Yu. G. Ptushinskii

*Institute of Physics of the National Academy of Sciences of Ukraine, pr. Nauki 46, Kiev 03028, Ukraine*

(Submitted July 12, 2004; revised September 28, 2004)

*Fiz. Nizk. Temp.* **31**, 300–322 (March–April 2005)

Results from simulations of the adsorption of gases on transition metal surfaces are presented. Attention is devoted mainly to the adsorption of hydrogen on the (110) surfaces of W and Mo, the structures and adsorption kinetics of oxygen and CO on the Pt(111) surface, and the catalytic reaction of CO oxidation. The choice of these systems is motivated not only by their practical importance and fundamental interest but also by the fact that substantial progress has been made toward understanding the processes of adsorption and the formation of film structures for them with the use of the Monte Carlo method. One of the main requisites for simulation of the adsorbed film structures is to adequately incorporate the lateral interaction between adsorbed molecules, which includes both a direct interaction (electrostatic and exchange) and indirect (via electrons of the substrate). The correct description of the lateral interaction in the simulation has permitted explanation of the mechanisms of formation of the structures of CO films on platinum. At the same time, the complexity of the interaction between adsorbed atoms has at yet precluded the development of a consistent model for the formation of the structure of adsorbed oxygen on the platinum surface. It can be hoped that this problem will soon be solved, making it possible to refine the model of the catalytic reaction of CO oxidation. © 2005 American Institute of Physics. [DOI: 10.1063/1.1884424]

### 1. INTRODUCTION

The basic principles of the modern concepts of the physics of adsorption were set forth back in the early twentieth century by Irving Langmuir. Despite the enormous progress in our understanding of the process of gas adsorption on various surfaces, many of its important details and interrelationships require clarification. Interest in the adsorption of gases on transition metals stems not only from the possible importance of such research (it suffices to mention the necessity of achieving further progress on the problems of heterogeneous catalysis, for example, the problem of removing pollutants from the exhaust gases of automobiles and the comprehensive decontamination of the atmosphere), but also from the possibility of carrying out multifaceted research on such adsorption systems for the purpose of obtaining new information about the properties of surfaces. For example, low-energy electron diffraction (LEED) and scanning tunneling microscopy (STM) are used to study the structure of the surface and of the adsorbed film, and photo- and x-ray-electron spectroscopy are used to study the electronic structure. Infrared spectroscopy yields information about the types of adsorption sites and bonds and their symmetry, and experiments on diffusion, temperature programmed desorption, particle scattering, and adsorption kinetics can determine the adsorption energy and binding force of the molecules and atoms with the surface.

Progress in research on the adsorption of gases on transition metals demands the use of novel comprehensive techniques in addition to conventional methods. For example, for studying molecular adsorption of hydrogen by the molecular beam method (for purposes of studying the adsorption kinetics and to obtain information about the interaction potential between the incoming particle and the solid surface) the sub-

strate must be cooled to liquid helium temperature. Obviously, purposeful investigation of the properties of adsorption systems also requires theoretical studies. Unfortunately, the possibilities for rigorous theoretical calculations of the interaction parameters of particles with metal surfaces are extremely limited because of the necessity of taking into account a large number of different factors, such as the presence of precursor states, accommodation, the character of the adsorption bond (ionic, covalent), the types of lateral interaction, and the rate of surface diffusion. Since many experiments on gas adsorption are done under equilibrium (or quasi-equilibrium) conditions, one can in principle employ thermodynamic methods to estimate the kinetic characteristics, but the accuracy of such estimates is insufficient for direct comparison with experimental data.

Using modern methods of calculation (in the framework of electron density functional theory) one can quite reliably estimate the binding energy of an atom or molecule with the surface, determine the most favorable adsorption centers, and estimate the interaction energy between adsorbed particles (the lateral interaction). However, significant difficulties arise when one attempts to compare the results of such model calculations with experimental data on adsorption. This to a large degree is due to the fact that experiments usually measure the integrated characteristics (sticking coefficient and diffusion coefficient, the heat of adsorption, etc.), whereas calculations give numerical values of the interaction parameters between particles and the surface and therefore cannot always be used directly for interpretation of the results of studies of the adsorption kinetics.

The complexity of calculations of the interaction with the surface for incoming gas molecules can be illustrated by the example of the so-called “six-dimensional potential

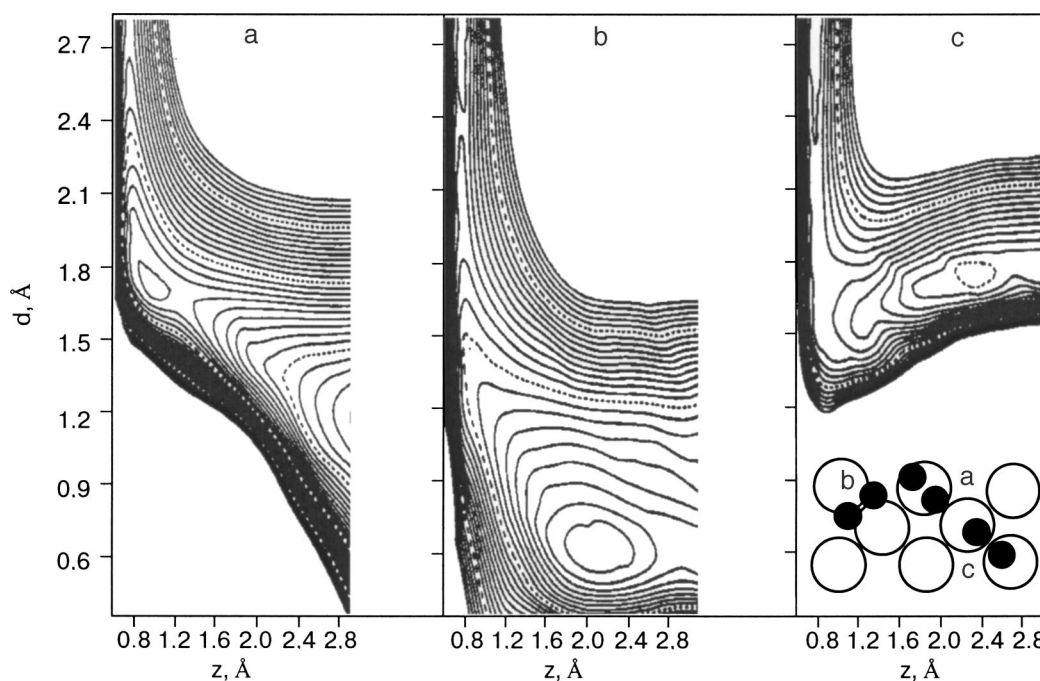


FIG. 1. Potential energy surfaces for hydrogen molecules on W(100) from Ref. 8: for molecules above an on-top center the axis of the molecule is parallel to the direction between two bridge positions on the substrate—barrierless desorption (a); for a molecule above a bridge adsorption center with the axis of the molecule parallel to the direction between two positions of threefold symmetry—barrierless desorption (b); for a molecule above a bridge position with the axis of the molecule parallel to the direction on the surface between two on-top positions (c). The barrier for desorption is 0.3 eV.

model.” The molecular dynamics method is used to calculate the forces of interaction with the surface for different orientations (and sometimes velocities) of the molecules, and potential energy surfaces (PESs) are constructed.<sup>1–7</sup> As an example, Fig. 1 shows the PES calculated in Ref. 8 for hydrogen on W(100). In this model the growth of the initial sticking coefficient with decreasing energy of the incident hydrogen molecule is explained by a decrease in the speed of rotation owing to an orientation (or steering) of the incoming molecule. As a result of steering the molecule is oriented with respect to the surface in such a way that the probability of breaking the molecular bond becomes maximum. Thus, if a molecule oriented along the surface approaches an on-top or bridge position on the surface there is no potential barrier for chemisorption. However, if the axis of the molecule is perpendicular to the surface, the molecule cannot be chemisorbed in an on-top site (the potential barrier in this case is practically infinite), while the barrier for chemisorption in the bridge position is 0.3 eV. For dissociative chemisorption of a molecule in a position of threefold symmetry a potential barrier exists for any orientation of the incoming molecule.

For describing probabilistic processes in systems with a large number of particles it is reasonable to make use of statistical simulation (the Monte Carlo method). The Monte Carlo method is widely used for studying the interaction of particles with a solid surface, crystal growth, adsorption, diffusion, and ordering of adsorbed atoms and molecules, and also chemical reactions on a surface. With this method one can do a computer experiment (simulation) based on physical concepts obtained as a result of experimental and theoretical studies of a given adsorption system. This not only allows one to check the correctness of existing ideas about the system but also to propose new concepts for interpreting

the experimental data and, in a number of cases, to predict the behavior of systems under some particular conditions or other.

In this review we discuss the possibilities of the Monte Carlo method and the prospects for its use in modeling the adsorption of gases on transition metals. We present and analyze the results of simulations of the low-temperature adsorption of hydrogen (with precursor states and the phenomenon of enhanced accommodation taken into account), adsorption, the formation of structures of adsorbed films of oxygen and CO on platinum, and the catalytic reaction of CO oxidation.

## 2. ROLE OF PRECURSOR STATES IN LOW-TEMPERATURE ADSORPTION OF HYDROGEN ON TRANSITION METALS

### 2.1. Accommodation of molecules and the initial sticking coefficient

The probability of adsorption of a molecule on a surface (the initial sticking coefficient) depends on the energy of the particle, the direction of incidence, and the temperature of the substrate. At a low substrate temperature the probability of physisorption is determined mainly by the efficiency of transfer of the kinetic energy of the molecules to atoms of the surface in collision (accommodation of the molecule), after which the molecule is trapped by the surface, where its energy is close to the value of the minimum of the van der Waals potential (see Fig. 2). Accommodation of the molecule is explained by the loss of energy to excitation of one or several phonons in the substrate and, in some cases, the formation of electron–hole pairs also.<sup>9</sup> For particles with low energies the second process has a low probability and is usu-

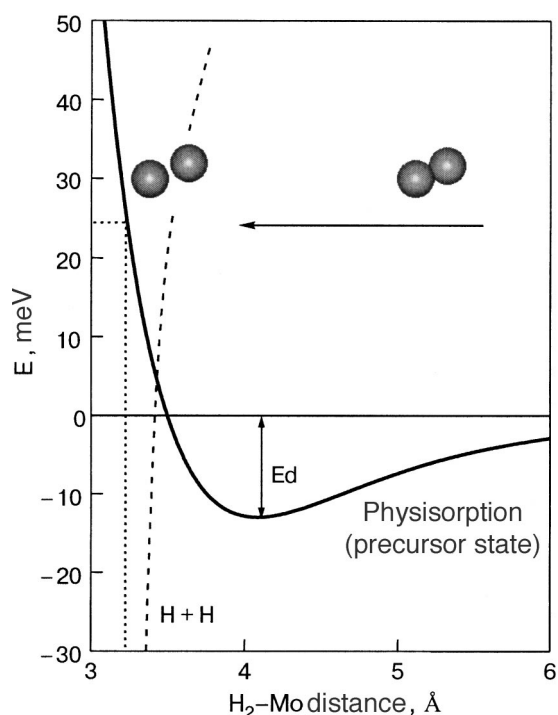


FIG. 2. One-dimensional interaction potential of a hydrogen molecule with the Mo(110) surface, calculated in the classical approximation.<sup>47</sup>

ally neglected. Taking a classical approach, one can estimate the scattering probability in the case of one- and two-phonon processes.<sup>9–13</sup> However, for typical energies of the hydrogen molecules in a molecular beam (25 meV) the scattering length has a value of the order of the lattice period on the surface of a transition metal, and that leads to significant diffraction effects.<sup>9</sup> Thus for a realistic description of the scattering of hydrogen molecules one must use a quantum-mechanical approach, which is practical only for a one-phonon process.<sup>9,13,14</sup> In Ref. 9 an analysis of the dependence of the sticking coefficient on the energy of the incident particle,  $S(E)$ , was done both from a classical standpoint and with quantum effects taken into account. It was shown that at low energies of the incident particles ( $E \rightarrow 0$ ) in the classical description  $S(E) \rightarrow 1$ , while in the case when quantum effects—in particular, quantum reflection—are included, the dependence has the form  $S(E) \sim E^{1/2}$  for neutral atoms.

Clearly the adsorption of hydrogen on a metal surface can substantially alter the surface contribution to the phonon spectrum of the system, and therefore the estimates made are only of a qualitative character. For example, in the adsorption of a monolayer of hydrogen on the W(110) and Mo(110) surfaces one observes anomalies in the scattering spectrum of He atoms in comparison with scattering on the clean surface.<sup>15</sup> Softening of a phonon mode is due to electron–phonon coupling, which is enhanced on account of adsorption-induced surface states. This explanation is confirmed by calculations of the atomic and electronic structure, the vibrational spectra, and the spectra of excitation of electron–hole pairs in these systems in the framework of density functional theory.<sup>16,17</sup> Unfortunately, the necessity of taking into account a large number of factors influencing the accommodation makes it impossible the estimate the initial

sticking coefficient to the accuracy necessary for comparison with experiment.

## 2.2. Precursor states and steering

Hydrogen can be adsorbed on transition metals in a process involving dissociation of the molecules and subsequent chemisorption of the individual atoms or at low temperatures in a weakly bound physisorbed molecular state.<sup>18–28</sup> The activation energy for dissociative chemisorption of hydrogen on W(110) and Mo(110), as follows from the growth of the sticking coefficient with decreasing energy of the incident molecules, is extremely insignificant, so that one can observe atomic chemisorption even at a temperature of 5 K. After an atomic layer is filled the further adsorption of hydrogen takes place in molecular form. The highest degree of coverage  $\theta$  by hydrogen at  $T = 5$  K in dynamic equilibrium with the incident hydrogen beam is  $\theta = 1.5$ , which corresponds to the formation of a complete molecular monolayer (ML) of hydrogen on top of the atomic monolayer (the degree of coverage is defined as the number of hydrogen molecules per adsorption site on the W(110) or Mo(110) surface, so that  $\theta = 0.5$  corresponds to a filled atomic monolayer).

The chemisorption barrier for hydrogen adsorption on noble metals (Au, Cu) and transition metals (Pd, Rh, Pt, W, Mo) are substantially different. For noble metals typically there is a high activation barrier for dissociation. In contrast, for hydrogen adsorption on Ni(111) and Pt(111) the activation barrier is 50–100 meV, and for hydrogen adsorption on Rh(111) activationless chemisorption of hydrogen is observed. The value of the barrier for dissociation of hydrogen is determined by the crossing of the repulsive part of the physisorption potential and the attractive region of the chemisorption potential for atomic hydrogen (see Fig. 2). The difference between the surface potentials of transition and noble metals is apparently due to their different electronic structure (especially the difference between the surface states).<sup>20,29–31</sup>

Apparently the mechanism of dissociative chemisorption consists in the following. Electrons of the substrate escaping to vacuum can occupy antibonding states of the molecule and cause its dissociation<sup>32,33</sup> and the subsequent chemisorption of the individual atoms. Obviously an important role in this is played by the intrinsic and extrinsic precursor states.<sup>10,22–25,34–37</sup> A molecule trapped in a precursor state can move along the surface and come upon a favorable adsorption site, and this leads to its dissociation and the chemisorption of the atoms at two adjacent adsorption centers. At the same time, a molecule trapped in a precursor state can also desorb, in contradistinction to the model of direct dissociative chemisorption.<sup>8,38–42</sup>

The existence of intrinsic precursor states is still in dispute. For highly activationless chemisorption, as is characteristic of the adsorption of hydrogen on simple and noble metals,<sup>11,12,42,43</sup> the existence of extrinsic precursor states is confirmed by the presence of both atomic and molecular hydrogen on the surface even at very low coverages. In this situation the molecular physisorbed state can serve as a precursor state for the subsequent dissociative chemisorption. Whereas dissociative adsorption of hydrogen is observed at

low energies of the incident molecules, the presence of intrinsic precursor states can be confirmed only indirectly.<sup>19–21,23,26–28,34–37,43</sup>

At the same time, the steering effect can account for some experimental data on the sticking coefficient of hydrogen without any need for invoking the concept of precursor states, and for that reason the existence of intrinsic precursor states has been called into question.<sup>44</sup> However, it follows from the calculations of Refs. 8 and 38–41 that the hydrogen molecules have a high mobility along the surface and thus spend a significant time near the surface before reflecting or dissociating.<sup>8,39–41</sup> Furthermore, the barrierless (direct) chemisorption of hydrogen on the W(100) surface, as follows from the calculations of Ref. 8, is observed only for certain orientations of the molecules with respect to the surface, and for other orientations this barrier is quite significant (see Fig. 1). Such a state in a two-dimensional model of the surface potential can be considered to be an intrinsic precursor state.<sup>18,29,45,46</sup> Thus the concept of precursor states as a temporary molecular state prior to chemisorption does not really contradict the steering-effect model, since in both models it is assumed that the molecule spends a significant time near the surface prior to its dissociation or return to the gas phase.

### 2.3. Effective two-dimensional potential

For qualitative description of the motion of a molecule it is advisable to use a one-dimensional potential model averaged over the surface. Two approaches are usually taken in the commonly used software packages based on methods of quantum chemistry: 1) classical Newtonian mechanics; 2) semiempirical potentials using universal parameters for the overlap integrals; 3) *ab initio* calculations (by the Hartree–Fock method, with the configuration interaction also taken into account if necessary), and 4) calculations using density functional theory. The interaction with the model surface can be described in terms of classical molecular mechanics or quantum mechanics. Quantum-mechanical calculations using the semiempirical approximation yield rather reliable estimates for the interaction parameters. In Newtonian mechanics the hydrogen molecule is treated as a classical particle in the fields of a van der Waals potential near the surface, while the semiempirical potential, which takes the electronic structure of the molecule into account, also permits modeling of its dissociation.

The interaction potential of the hydrogen molecule with the Mo(110) surface, calculated in the classical approximation, is shown in Fig. 2.<sup>47</sup> A particle approaching the surface is attracted by the van der Waals forces to a distance at which it begins to feel the “tail” of metal electrons escaping to vacuum. The interaction with these electrons leads to the formation of a repulsive potential and can lead to reflection of the particle. However, the molecule may lose kinetic energy (e.g., owing to excitation of phonons in the substrate)<sup>9–13</sup> and, as a result, be trapped in a potential near the surface, corresponding to a state of physical adsorption. The depth of the physisorption well for hydrogen on Mo(110) is only around 15 meV,<sup>47,20</sup> and therefore a stable molecular layer of physisorbed hydrogen can be obtained only at low substrate temperatures.

### 2.4. Monte Carlo simulation of adsorption kinetics of hydrogen

In both physical and chemical adsorption the atoms and molecules generally occupy certain sites or adsorption centers. This position is determined by the interaction potential of the particle with the surface, and it is therefore logical to assume that the geometry of the arrangement of adsorption centers is determined by the potential relief of the surface. Indeed, in an atomic adsorbed layer the limiting concentration of hydrogen atoms is equal to the surface concentration of atoms of the substrate, which can present as a lattice of adsorption centers, each of which can be occupied by one atom. Clearly the presence of an atomic layer on a surface can influence the binding of the molecules of the second layer with the surface. Nevertheless, the molecular adsorption of hydrogen can also be described by a lattice-gas model, inasmuch as it has been observed in experiment that the second (molecular) layer is saturated at the same concentration of hydrogen molecules as the surface concentration of substrate atoms. This feature allows one to describe the molecular and dissociative adsorption of hydrogen by the Monte Carlo method, which gives a transparent description of the process and enables one to elucidate the role of the various factors influencing the effective sticking coefficient.

It has been observed in molecular beam experiments at low temperatures (5 K) that the adsorption kinetics of hydrogen demonstrates a strong dependence of the sticking coefficient  $S$  and of the limiting dynamic-equilibrium coverage on the molecular flux.<sup>28</sup> For example, at high fluxes a significant maximum of  $S$  is observed at coverages in the region corresponding to molecularly adsorbed hydrogen, while at low fluxes this maximum is very slight or absent altogether. Furthermore, the limiting equilibrium coverage at high fluxes equals 1, while at low fluxes it is 0.2.

The dependence of the sticking coefficient on the degree of coverage is given by the relation

$$S(\theta) = 1 - k(\theta) - \theta n_0 W(\theta)/F, \quad (1)$$

where  $\theta$  is the degree of coverage, defined as  $\theta = n/n_0$  [ $n_0$  is the density of adsorption sites,  $1.4 \times 10^{15} \text{ cm}^{-2}$  in the case of the W(110) or Mo(110) surface],  $k(\theta)$  is the coefficient of reflection of a molecule from the surface,  $W(\theta) = \nu \exp(-E_{\text{eff}}/k_b T)$  is the desorption probability,  $E_{\text{eff}} = E_d + U$  ( $E_d$  is the activation energy for desorption,  $U$  is the energy of the lateral interaction of neighboring atoms),  $\nu$  is the frequency factor, and  $F$  is the particle flux. The influence of the flux on  $S(\theta)$  is explained by enhancement of the accommodation for particles that in the process of their adsorption collide with previously adsorbed molecules.<sup>48–51</sup> Indeed, in the collision of a molecule with a heavy substrate atom, because of the mass mismatch of the colliding particles, it is harder for a molecule to lose sufficient energy to become trapped in the physisorption well, and upon collision with an already adsorbed molecule, owing to the equality of the masses, the exchange of energy will be much more efficient, and therefore the probability of adsorption will be higher. The situation can be modeled as follows. If a molecule collides with a substrate atom, then the probability of adsorption is determined by the initial sticking coefficient  $S_0$  (the simulation can be done using the value of  $S_0$  obtained from ex-

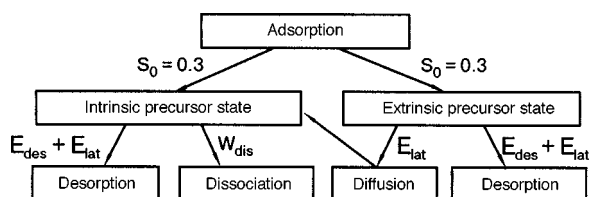


FIG. 3. Scheme of the simulation of adsorption of hydrogen on a transition metal.

periment), while if it collides with an adsorbed molecule when an unoccupied adsorption site is among the nearest neighbors, then the adsorption probability is taken equal to unity.

The scheme of the Monte Carlo simulation of hydrogen adsorption in Ref. 47 was as follows (Fig. 3):

1. An adsorption center is selected at random. If the center is unoccupied or occupied by a chemisorbed atom, then the molecule with a certain probability  $W_A$  (determined by the initial sticking coefficient  $S_0$ ) is trapped in an intrinsic or extrinsic precursor state, respectively.

2. A molecule trapped into this precursor state can either dissociate (with a probability  $W_{\text{diss}}$ ) with the instantaneous chemisorption of the hydrogen atoms (in the presence of an unoccupied adsorption center) or can make several diffusion hops or be desorbed. At low coverages and low temperatures desorption of a molecule is considerably less probable than diffusion, and the desorption of atoms from a chemisorbed state is practically impossible at low temperatures.

3. If the chosen center is occupied by a molecule, than it is assumed that the accommodation of molecules in this case is significantly enhanced on account of the equality of the particle masses. This circumstance is taken into account with the aid of a modeling of the possibility for such a molecule to occupy the nearest center not occupied by another molecule, and in that case the desorption probability is equal to 1.

The result of the Monte Carlo simulation of hydrogen adsorption on W(110) and Mo(110) with diffusion and the lateral interaction between molecules and also the enhanced

accommodation<sup>45</sup> taken into account is in good agreement with the experimental  $S(\theta)$  curves in the entire range of coverages studied and at all values of the flux of hydrogen molecules (Fig. 4a). The calculated  $S(\theta)$  curve reproduces well such experimentally observed features as enhancement of sticking and growth of the limiting dynamic-equilibrium coverage with increasing flux of hydrogen molecules onto the surface. The growth of the sticking coefficient with increasing flux here is due to the enhanced accommodation for the hydrogen molecules at high fluxes, and the increase in the limiting coverage is due to a change in the ratio of the desorption flux to the incident flux [see Eq. (1)]. It should be noted that in using this model it is unnecessary to include other parameters in order to get the growth of the sticking coefficient at high coverages and fluxes. Such agreement with the experimental data can be obtained only if the role of the intrinsic and extrinsic precursor states is adequately taken into account. For example, control calculations of the functions  $S(\theta)$  without the precursor states have revealed the absence of experimentally observable dependence of the sticking coefficient on the flux at coverages of around 0.5 (Fig. 4b).

For hydrogen adsorption on Mo(110) the dependence of the sticking coefficient on the degree of coverage is qualitatively different from the case of  $\text{H}_2$  adsorption on W(110) and of deuterium adsorption on Mo(110). Only for the system H/Mo(110) is a sharp decrease of the sticking coefficient observed at coverage  $\theta=0.5$  (Fig. 5). In Refs. 27 and 52 this difference in the behavior of  $S(\theta)$  was explained by the anomalously high mobility of hydrogen on Mo(110). On the basis of the results of a simulation<sup>47</sup> an alternative explanation was proposed for the different behavior of  $S(\theta)$  in the cases of hydrogen and deuterium adsorption on Mo(110). For example, when only the difference of the activation energies for desorption of hydrogen and deuterium on Mo(110) is taken into account, one observes a tendency to form a minimum (Fig. 5).

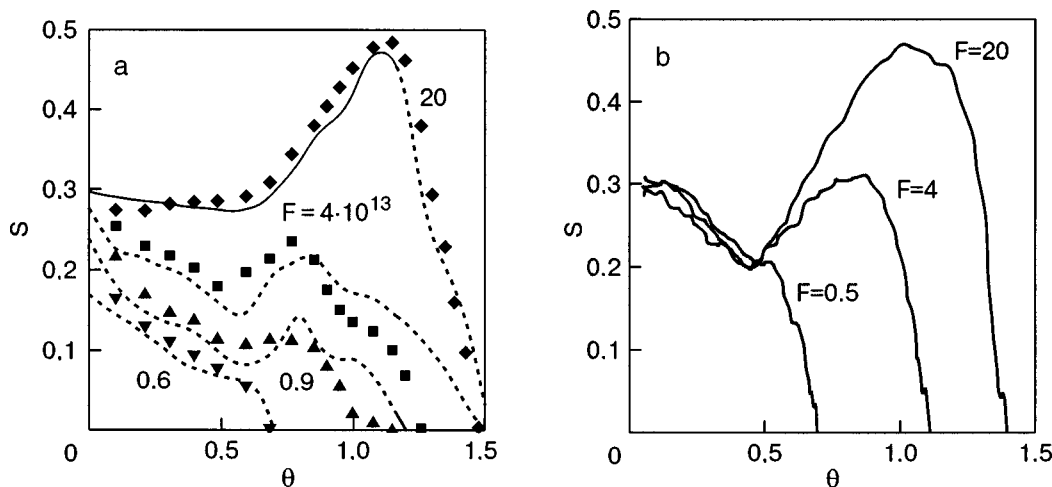


FIG. 4. Dependence of the sticking coefficient of hydrogen on W(110) on the degree of coverage for different values of the incident particle flux (the dashed curves show the experimental results, and the symbols the result of a simulation<sup>47</sup> including precursor states) (a); the results of a simulation for different fluxes in the case of direct chemisorption (b).

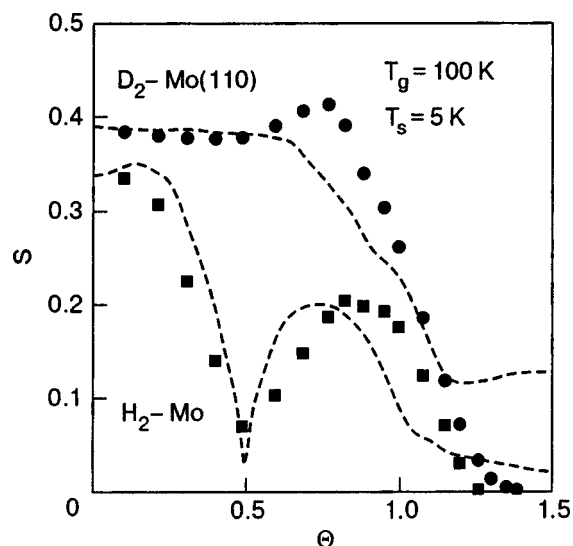


FIG. 5. Dependence of the sticking coefficient on the degree of coverage for hydrogen and deuterium on Mo(110) (the dashed curve is experimental, the symbols the results of a simulation<sup>47</sup>).

### 2.5. Simulation of hydrogen desorption

An effective method for investigating the interaction of an adsorbate with a surface is temperature programmed desorption (TPD). For interpretation of the TPD spectra one usually uses the Polanyi–Wigner equation for the rate of desorption:

$$R_{\text{des}} = \theta^n \nu \exp(-E_{\text{eff}}/k_B T),$$

where  $R_{\text{des}}$  is the rate of desorption,  $\nu$  is a pre-exponential

factor,  $E_{\text{eff}} = E_{\text{des}} + E_{\text{lat}}$  is the effective activation energy for desorption with the lateral interaction taken into account, and  $n$  is the order of desorption.<sup>53,54</sup>

The presence of the lateral interaction between adsorbed particles has a sensitive influence on the position of the peaks in the TPD spectrum. A Monte Carlo simulation of the desorption process in real time permits one to determine the influence of the lateral interaction on the position and shape of the TPD peaks and also to estimate the value of this interaction. In Ref. 55 an algorithm was proposed for Monte Carlo simulation of the TPD spectra in real time and to analyze the influence on the TPD spectra of the substrate geometry and the lateral interaction between particles. It was shown that the presence of a repulsive interaction leads to the appearance of two peaks in the TPD spectra, corresponding to desorption from different ordered phases on the surface, the larger splitting of the peaks corresponding to the stronger lateral repulsion. For a weak repulsion one observes some broadening of the desorption peak. The presence of an attractive interaction for the next-nearest neighbors when the nearest neighbors have a repulsive interaction leads to sharpening of the TPD peak. In Ref. 45 a simulation of the TPD and isothermal desorption spectra of the system  $\text{H}_2/\text{W}(110)$  was done for the cases of different initial degrees of coverage (see Fig. 6). The values obtained for the activation energy of desorption and the lateral interaction from the results of a simulation<sup>45</sup> for the systems  $\text{H}_2/\text{W}(110)$ ,  $\text{H}_2/\text{Mo}(110)$ , and  $\text{D}_2/\text{W}(110)$  are in good agreement with experiment, and so the algorithm developed can be used for simulation of the adsorption and desorption processes for the different systems and can also be used to explain the coverage dependence of the sticking coefficient of CO and oxygen on Pt(111), the

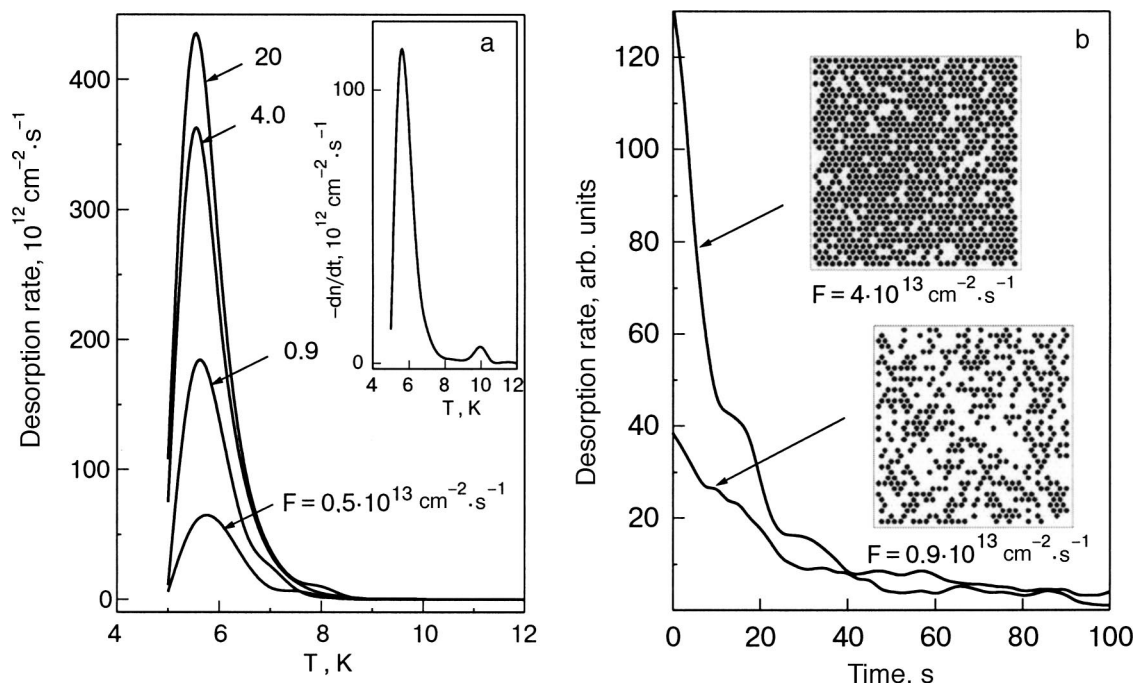


FIG. 6. Temperature programmed desorption (TPD) spectrum for the system  $\text{H}_2/\text{W}(110)$ , obtained as a result of the simulation for different fluxes (the inset shows the TPD spectrum obtained in an experiment<sup>26</sup> at a molecular flux  $F = 0.9 \times 10^{13} \text{ cm}^{-2} \text{ s}^{-1}$ ) (a); the distribution of the hydrogen molecules at the equilibrium coverages on W(110), obtained for  $F = 0.9 \times 10^{13}$  and  $4 \times 10^{13} \text{ cm}^{-2} \text{ s}^{-1}$  and the spectra of isothermal molecular desorption (in relative units), obtained as a result of a simulation<sup>45</sup> for 5 K (b).

structural ordering of adsorbed CO molecules,<sup>56</sup> and the catalytic reaction of CO oxidation on the platinum surface.

### 3. SIMULATION OF THE CO OXIDATION REACTION ON Pt(111)

A huge number of studies devoted to the adsorption of CO on platinum is due not only to the importance of the development of fundamental concepts but also to the search for possible ways of perfecting platinum catalysts for removing pollutants from the exhaust gases of automobiles. The catalytic reaction of CO oxidation takes place by the Langmuir–Hinshelwood mechanism (a bibliography may be found in Imbihl's excellent review<sup>57</sup> of oscillatory reactions on the surfaces of single crystals). Clearly the electronic and catalytic properties depend substantially on the structure of the substrate surface and of the adsorbed layer. From a practical standpoint the surface of greatest interest is that of polycrystalline Pt, which on annealing acquires a (111) texture. This fact accounts for the significant interest in studying the adsorption of CO and the joint adsorption of CO and oxygen on specifically the Pt(111) surface.<sup>58–67</sup>

For simulation of the catalytic reaction of CO oxidation on the platinum surface the Monte Carlo method with the ZGB algorithm, proposed by Ziff, Gulary, and Barshad,<sup>68</sup> is widely used. This mechanism consists in the following: 1) in accordance with the relative concentration of the gas in the mixture the choice of a candidate for adsorption—CO or O<sub>2</sub>—is made; 2) an unoccupied adsorption center is selected at random and is filled in the case of CO adsorption or is filled together with an adjacent unoccupied adsorption center in the case of oxygen adsorption; 3) in the case when the CO molecule and an O atom occur in adjacent adsorption centers on the surface, a reaction takes place between them (with the instantaneous evaporation of CO<sub>2</sub>), and both adsorption centers become unoccupied. The results of a calculation in this model give a strictly bounded region of relative pressures of CO in which a reaction is possible:  $P_{\text{CO}}/P_{\text{O}_2} = 0.39\text{--}0.53$ . To the left of this region the model predicts poisoning of the surface by oxygen, and to the right, by CO. Experimentally, however, poisoning of the platinum surface by oxygen is not observed, and the degree of suppression of the reaction because of CO adsorption is strongly temperature dependent.

Thus the given algorithm has a number of important shortcomings, and for that reason several refined versions have been proposed to take into account the parameters of the diffusion, desorption of CO, and lateral interactions in the system.<sup>69–72</sup>

In Refs. 70 and 72 the Monte Carlo method was used to investigate the influence of desorption and diffusion of CO molecules on the characteristics of the hysteresis in the CO oxidation reaction. In particular, it was shown that the diffusion of CO leads, on the one hand, to separation of the unoccupied pairs of adsorption sites needed for adsorption of oxygen, and thereby decreases its adsorption probability. On the other hand, diffusion increases the probability of the CO<sub>2</sub> formation reaction, which leads to a decrease of the amount of oxygen on the surface. In addition, the presence of diffusion leads to significant broadening of the hysteresis loop in the dependence of the reaction rate on the CO partial pressure. The presence of CO desorption is also one of the

mechanisms that empty the adsorption sites for subsequent adsorption of reactants, and the increase of the CO desorption probability leads to narrowing of the hysteresis loop.

It should be noted that the factors listed still do not avoid the oxygen poisoning of the surface that is obtained in the ZGB model. For this reason the algorithm used to describe the adsorption kinetics was substantially modified in Ref. 67. As a result, the dependence of the CO oxidation reaction rate on Pt(111) on the relative pressure of CO was found to be in good agreement with experiment for the entire range of relative pressures of the reactants. The influence of lithium adsorption on the course of the CO oxidation reaction on the Pt(111) surface was investigated in that paper. It was shown that because of their small size, Li adatoms occupy the active centers on the surface, leading to an effective decrease of its area. At the same time, the possible enhancement of oxygen adsorption at low Li coverages is small because of the small value of the dipole moment of the adatoms. At close to monolayer coverages, when the mutual depolarization of the dipoles causes metallization of the adsorbed Li layer, the rate of oxygen adsorption decreases rapidly, as a result of which the oxidation reaction is suppressed. The validity of this qualitative explanation of the role of Li in the reaction has been confirmed by Monte Carlo simulation of the reaction with the use of the ZGB model. Besides desorption and diffusion of the CO molecules, the probability of oxygen adsorption was also taken into account in the model, by the introduction of an initial sticking coefficient taken from experiment. In contrast to the usual way of modeling the desorption probability,<sup>68,72,73</sup> in this model an attempt at desorption was made whenever there was no attempt at adsorption because the site was occupied. Thus an implicit description of the growth of desorption with increasing degree of coverage is achieved. Incorporation of a sticking coefficient as well as desorption and diffusion made it possible to obtain good agreement between the calculated and experimental dependence of the reaction rate on the relative pressure of CO (Fig. 7). Here it should be noted that the calculated position of the maximum rate agrees with the experimentally observed rate at  $T=480$  K, a feat that had not been achieved previously in a simulation of the reaction on the Pt(111) surface.<sup>72</sup>

The adsorption of alkali metals was incorporated in the simulation with the assumption that they occupy the same adsorption sites as CO and O. The influence of an alkali metal on the adsorption of oxygen is described by a corresponding change of the initial sticking coefficient. The results of the simulation for different Li coverages are presented in Fig. 7. Despite the increase of the initial sticking coefficient for oxygen in the presence of Li, which leads to a shift of the reaction rate maximum to higher CO relative pressures, the reaction rate falls off rapidly with increasing Li coverage. Thus it was shown<sup>67</sup> that the influence of Li on CO oxidation on the Pt(111) surface presupposes the existence of two competing effects: the increase of the sticking coefficient for oxygen (aiding the reaction) and, on the other hand, a decrease of the number of adsorption centers, which leads to a decrease of the CO and oxygen adsorption probabilities.

Nevertheless, in all the studies mentioned on the subject

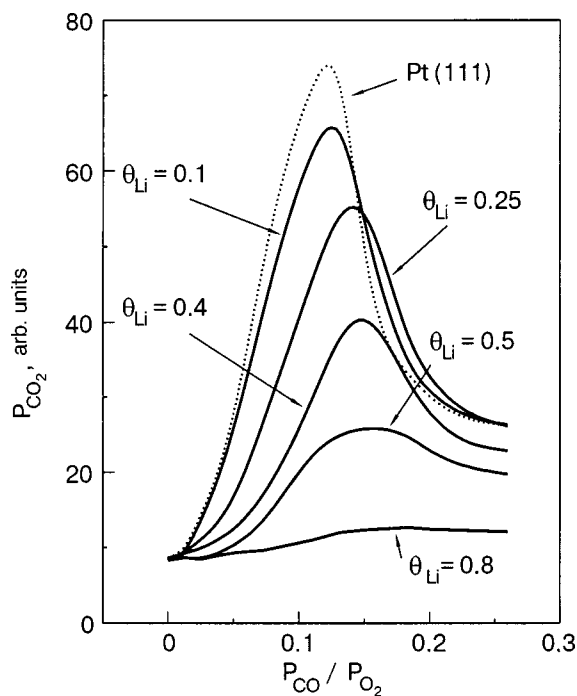


FIG. 7. Results of a simulation<sup>67</sup> of the CO oxidation reaction on the Pt surface in the presence of Li at a temperature of 480 K.  $P_{CO_2}$ ,  $P_{O_2}$ , and  $P_{CO}$  are the partial pressures of the components in the gas phase,  $\theta_{Li}$  is the degree of coverage by Li on Pt(111).

of simulation of the CO oxidation reaction on the platinum surface it was impossible to obtain the correct values of the maximum coverages in the limiting cases of separate adsorption of oxygen or CO. Consequently, the algorithm used in simulation of the reaction is in need of further refinement, which can be achieved with a more realistic description of both the lattice of adsorption centers on the surface and the lateral interaction between molecules.

#### 4. STRUCTURE FORMATION AND ADSORPTION KINETICS OF CO ON Pt(111)

The CO film structures formed at different coverages on Pt(111) have been investigated in a number of studies and, it would seem, the basic rules governing adsorption and the sequence of structures formed with increasing coverage should be well established. For example, it was found by Ertl *et al.*<sup>58</sup> that at coverage  $\theta=1/3$  a  $(\sqrt{3}\times\sqrt{3})R30^\circ$  structure is formed. This structure is observed only at reduced temperatures (170 K)<sup>59</sup> and is practically absent at room temperature.<sup>58,59</sup> However, it is stated in Ref. 60 that the diffuse reflections of the  $(\sqrt{3}\times\sqrt{3})R30^\circ$  structure, which is observed at 100 K even at considerably lower coverages, are split and actually correspond to a more complex film structure.

At  $\theta=0.5$  a diffraction pattern (Fig. 8) corresponding to a well-ordered structure of the CO film on Pt(111) is observed even at room temperature. The observed diffraction pattern is usually interpreted,<sup>59–65</sup> following Ref. 58, as the formation of  $c(4\times 2)$  structure of the adsorbed film. It should be noted that similar diffraction patterns for CO on the similar surface Cu(111) were interpreted in Ref. 74 as the formation of the  $(1.5\times 1.5)R18^\circ$ , which corresponds to the

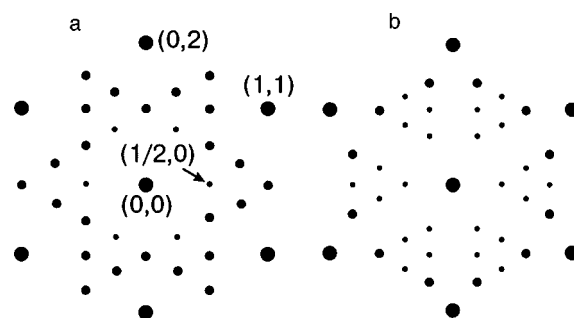


FIG. 8. Diagrams of the arrangement of reflections on the diffraction patterns for CO on Pt(111) at  $\theta=0.5$  (a) and  $0.6$  (b).<sup>58,59</sup> The different diameters of the circles correspond to different intensity of the reflections.

stoichiometric concentration  $\theta=0.44$ . On the Ni(111) surface<sup>75–81</sup> at coverage  $\theta=1/3$  the  $(\sqrt{3}\times\sqrt{3})R30^\circ$  structure forms, as on Pt(111), and for  $\theta=0.5$  the  $c(4\times 2)$  structure, but upon further increase in coverage the CO film takes on the structure  $(\sqrt{7}/2\times\sqrt{7}/2)R19.1^\circ$ , which differs from the structure observed on Pt(111) (see Fig. 8). The  $(\sqrt{3}\times\sqrt{3})R30^\circ$  structure is also observed in the adsorption of CO on the hexagonal faces Rh(111) (Refs. 29, 82, and 83) and Ru(0001) (Refs. 84 and 85).

Since the Pt(111) surface has a hexagonal structure, the structure of the adsorbed films is usually also designated in terms of the size and orientation of the experimental lattice with respect to the substrate.<sup>58,82</sup> In a number of cases, however, a rectangular cell can be chosen in the adsorbed layer, and then it is more convenient to use a notation in which the size of the unit cell and the number of particles in it are indicated explicitly.<sup>78</sup> Thus another notation for the structure  $c(4\times 2)$ , which contains two CO molecules in the unit cell ( $\theta=0.5$ ), is  $c(2\times\sqrt{3})rect$  [under the condition that the CO molecules at the center of the rectangular unit cells of size  $2a\times\sqrt{3}a$ ] or  $(2\times\sqrt{3})rect-2CO$ . In these systems of notation the structure of a CO film on Pt(111) at  $\theta=0.6$  (the maximum stable coverage for this system at a temperature of 160 K)<sup>59</sup> is characterized as  $c(5\times\sqrt{3})rect-3CO$ .

There is also disagreement<sup>48,59,74–80</sup> as to the type of adsorption centers occupied by CO molecules at different coverages on Pt(111) and Ni(111). For example, in some papers it is stated that the CO molecules on Ni(111) occupy positions at the centers of triangles formed by surface atoms,<sup>77</sup> while in other papers<sup>78</sup> it is emphatically argued that the CO molecules lie above substrate atoms and in bridge positions between two surface atoms. The situation with the adsorption of CO on Pt(111) is somewhat more definite in this regard. For Pt(111) the most reliably justified model is apparently one in which the filling of centers with increasing CO coverage occurs in the following order. Below a coverage  $\theta=0.33$  adsorption centers corresponding to the on-top position are filled.<sup>59,61–66</sup> With increasing coverage the bridge centers are also filled, and a redistribution of molecules occurs such that at  $\theta=0.5$  the number of occupied on-top centers is equal to the number of occupied bridge centers.<sup>59,61,85–87</sup> Such a sequence of filling of adsorption centers follows both from theoretical estimates<sup>62–66</sup> and from the data of a vibrational spectroscopy study<sup>61</sup> of CO on Pt(111).

It is reliably established (see, e.g., the review<sup>57</sup> and references cited therein) that on the Pt(111) surface the CO molecules stand vertically, with the oxygen atom upward, and thus their dipole moments are oriented parallel to each other. The adsorption of CO on Pt(111) causes an initial decrease of the work function,<sup>58,60</sup> i.e., CO acts as an electro-positive adsorbate. An estimate by the Helmholtz formula gives a dipole moment  $\mu \approx 0.2$  D [the intrinsic dipole moment of the bond in the CO molecule is 0.74 D for a single bond (C–O) and 2.3 D for a double bond (C=O)]. Hence it follows that the lateral interaction between CO molecules will have the character of dipole–dipole repulsion. The presence of repulsion between adsorbed CO molecules is also attested to by the decrease of the heat of adsorption with increasing coverage<sup>58</sup> and also by the a number of theoretical estimates.<sup>62–66,85–87</sup> At the same time, the formation of complex structures in the films and also an analysis<sup>88</sup> of the phase diagrams of the oxidation reaction of CO on Pt(111) indicates the presence of attraction between the adsorbed CO molecules at certain distances between them.<sup>84–87</sup> This long-range attraction is apparently due to the so-called indirect interaction,<sup>89–91</sup> i.e., the interaction of CO molecules via electrons of the substrate. The mutual depolarization of neighboring dipoles with increasing concentration on the surface also leads to a change of the value and character of the interaction, and at small distances between adsorbed molecules the direct exchange interaction between them also becomes important.<sup>63,89–91</sup>

Thus the interaction between adsorbed CO molecules on Pt(111) has a complex, nonmonotonic character and depends substantially on the coverage. In this situation the reliability of the interpretation of experimental data can be improved significantly by the use of mathematical simulations.<sup>48,55,92–97</sup> After a particular character of the lateral interaction is conjectured on the basis of an analysis of the sequence of structures observed in the adsorbed films, the reproduction of these structures in the mathematical simulation can be achieved. For this one should obviously choose the appropriate interaction parameters, which are determined on the basis of the requirement that the properties obtained match those observed in experiment.

#### 4.1. Interpretation of the diffraction patterns for CO on Pt(111)

Whereas the diffraction pattern at a CO coverage  $\theta = 0.33$  on Pt(111) or Ni(111) clearly corresponds to the  $(\sqrt{3} \times \sqrt{3})R30^\circ$  structure with the CO molecules at equivalent adsorption centers, the interpretation of the patterns for  $\theta = 0.5$  and 0.6 (see Fig. 8) is ambiguous and remains in dispute.<sup>58–65</sup> The point of contention is that the position of the reflections is determined by the symmetry of the two-dimensional lattice of the structure, while the distribution of the intensity of the reflections is determined by the position of the molecules in the unit cell. The lattice corresponding to the LEED pattern for  $T=0.5$  can be designated as  $c(4 \times 2)$  or  $(\sqrt{e} \times 2)rect$ , but in that case for one atom in the unit cell a coverage  $\theta=0.25$  is obtained. To see that such a structure gives the correct distribution of reflections in the diffraction pattern, one can estimate the relative influence of the low-energy electron reflection:

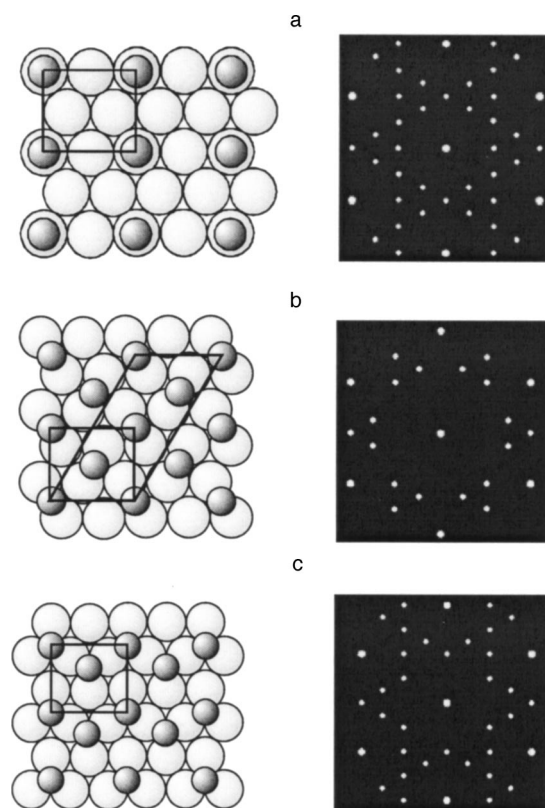


FIG. 9. Position of the atoms in a two-dimensional lattice with component  $c(4 \times 2)$  ( $\theta=0.25$ ) and the calculated diffraction pattern for the three equivalent orientations of such a lattice (a). The structure proposed for explaining the diffraction pattern observed<sup>58</sup> in CO films on Pt(111) (b). The structure of CO on Ni(111) proposed in Ref. 77 for  $\theta=0.5$  (c). The large, light circles represent atoms of the metal, and the small, dark circles represent CO molecules.

$$I(h,k) = \left| \sum_n \exp\{2\pi i(hx_n + ky_n)\} \right|^2 \quad (2)$$

and obtain the simulated diffraction pattern (Fig. 9a). The summation in this formula is over discrete coordinates of the molecules, expressed in fractions of the size of the simulated part of the surface, and  $h$  and  $k$  denote the coordinates in a two-dimensional reciprocal space. For a hexagonal lattice the strong reflections of electrons is obtained only when the sum of  $h$  and  $k$  is equal to an even number. By choosing arbitrary values of  $h$  and  $k$  one can model the intensity distribution on the screen of the LEED display.<sup>93,98,99</sup> Here one can trace the transformations of the patterns during the ordering of the structures and, if the step is chosen small enough, the variation of the width of the reflection upon variation of the size of the islands or the size of the simulated part of the surface (in Ref. 56 a part of the Pt(111) surface containing  $36 \times 30$  atoms and approximately  $100 \times 100$  Å in size<sup>99</sup> was chosen, corresponding to the coherence length for the standard LEED device).

An imitation of the LEED patterns was done by the following method. To indicate the brightness the reflections are represented by circles of radius proportional to the relative intensities of the electron reflection estimated by formula (2). For clarity the reflections coinciding with reflections from the substrate are represented by circles of slightly larger diameter.

An important feature of the LEED pattern calculated for the three equivalent orientations of the  $c(4 \times 2)$ , or  $(2 \times \sqrt{3})rect$ , structure ( $\theta=0.25$ ) (Fig. 9a), is the equality of the intensities of all 6 additional reflections forming the characteristic triangles. It is expected that the addition of molecules to the unit cell might lead to a decrease of the relative intensity of certain reflections owing to the effect of the structure factor. In particular, the reflection  $(1/2, 0)$  on the experimental patterns for  $\theta=0.5$  is considerably weaker than the other reflections (see Fig. 8), and this property can serve as an indicator of the correctness of the choice of unit cell.

Figure 9b,c shows the structures proposed in Refs. 58, 76, and 77 for explanation of the diffraction patterns observed in CO films on Pt(111) and Ni(111) at  $\theta=0.5$  (a diagram of the disposition of the reflections for this pattern is shown in Fig. 8). As is seen in the figure, the diffraction patterns calculated for all three orientations of the lattices are substantially different from those observed in experiment. Because of the location of the CO molecules at the center of the rectangular unit cell,<sup>58</sup> some of the experimentally observed reflections are suppressed by the structure factor and vanish from the pattern. We note that an analogous calculation<sup>77</sup> for this structure for CO and Ni(111) gave exactly the same results, since the diffraction pattern is obviously not affected by a displacement of the adsorbed layer such that the molecules occupy the positions characteristic for Ni(111), at centers with threefold symmetry. Nor is the situation rescued by displacement of the molecules along a symmetry axis of the rectangle—certain reflections vanish, as before. In Ref. 77 these missing reflections were artificially drawn in as if they were reflections appearing as a result of multiple reflection, which cannot be taken into account in the kinematic approximation. However, in the experiments of Refs. 58–60 these reflections were only slightly weaker than the others and can scarcely be due to multiple reflection. In order to obtain a diffraction pattern corresponding to the experimental one at  $\theta=0.5$  it is necessary to displace the CO molecules from the symmetric position. To preserve equality of the number of molecules in the two types of adsorption centers, on-top and bridge, it is advisable to consider the movement of molecules from the bridge positions at the center of the cells to the neighboring bridge centers (Fig. 10a). The choice of such centers is dictated by the following considerations. First, symmetry of the unit cell in even one direction inevitably leads to suppression of the corresponding reflection, and therefore the cell should be completely asymmetric. Second, the disposition of two molecules in the on-top position and the bridge center nearest to it is improbable because the minimum distance observed for adsorbed CO molecules ( $3.2\text{--}3.4 \text{ \AA}$ )<sup>58,59</sup> is considerably greater than the distance between such centers ( $1.38 \text{ \AA}$ ). Satisfaction of these requirements leads to the situation that when the corner molecules are placed in a rectangular unit cell at on-top centers, the proposed structure of the CO film on Pt(111) for  $\theta=0.5$  (Fig. 10a) is actually the only one possible (the disposition of molecules at the other three analogous centers, which corresponds to reflections in the symmetry planes of the rectangle, leads to equivalent unit cells). Each of the three possible orientations of the lattice corresponds to 2 pairwise symmetric unit cells, so that 6

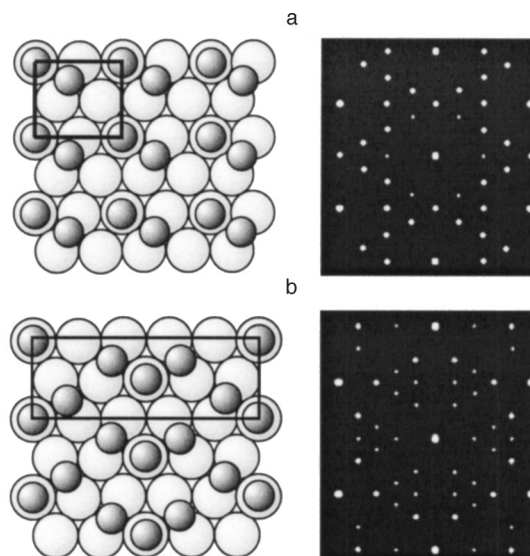


FIG. 10. The  $(2 \times \sqrt{3})rect$ -2CO structure of a CO film on Pt(111) for  $\theta=0.5$ .<sup>56</sup> The molecules at the corners of the rectangular unit cell are located at on-top centers, while those inside the rectangle are located at bridge positions. There are 6 equivalent domains of this structure which contribute to the diffraction pattern (right-hand panel) (a). The  $c(5 \times \sqrt{3})rect$ -3CO film of CO on Pt(111) for  $\theta=0.6$  (b).

equivalent domains (and not 3, as in the case of a centered cell) contribute to the diffraction pattern. For this reason the calculated diffraction pattern (Fig. 10a) is in excellent agreement with the experimentally observed pattern not only in respect to the distribution of superstructural reflections but also their relative intensities. In particular, reflections of the type  $(1/2, 0)$  in the bases of the characteristic triangles turn out to be noticeably weaker than the rest, as is well seen on the experimental patterns for CO on Pt(111) at  $\theta=0.5$ .<sup>58–60</sup>

Thus the proposed model of the structure of a CO film on Pt(111) at  $\theta=0.5$  can explain the observed diffraction patterns without the need for invoking addition assumptions involving multiple reflection. The correctness of the choice of asymmetric unit cell is also indicated by recent STM observations for the similar system CO on Ni(111) at  $\theta=0.5$ . The STM patterns presented in Ref. 78 clearly reveal the asymmetry of the unit cell, although the authors interpret it as the symmetric cell structure  $c(4 \times 2)$ , explaining the asymmetry as instrumental distortions.

At a degree of coverage  $\theta=0.6$  the diffraction pattern observed in experiment is obtained by adding the contributions from the six domains of the  $c(\sqrt{5} \times \sqrt{3})rect$ -3CO structure, illustrated in Fig. 10b. The CO molecules at the center and corners of the rectangular unit cell are located in on-top adsorption centers, while the rest are in bridge positions. Interestingly, this structure of the CO film on Pt(111) at  $\theta=0.6$  is observed by the addition of a third molecule to the characteristic pair of molecules at a distance  $a\sqrt{3}/2$ .

#### 4.2. Monte Carlo simulation of the ordering of a structure

At first glance it seems that the dipole–dipole interaction between adsorbed molecules is in itself sufficient to bring about the formation of the  $(\sqrt{3} \times \sqrt{3})R30^\circ$  structure, since this structure is most rarefied at  $\theta=0.33$ . However, the small value (0.2 D) of the dipole moment  $\mu$  estimated from the

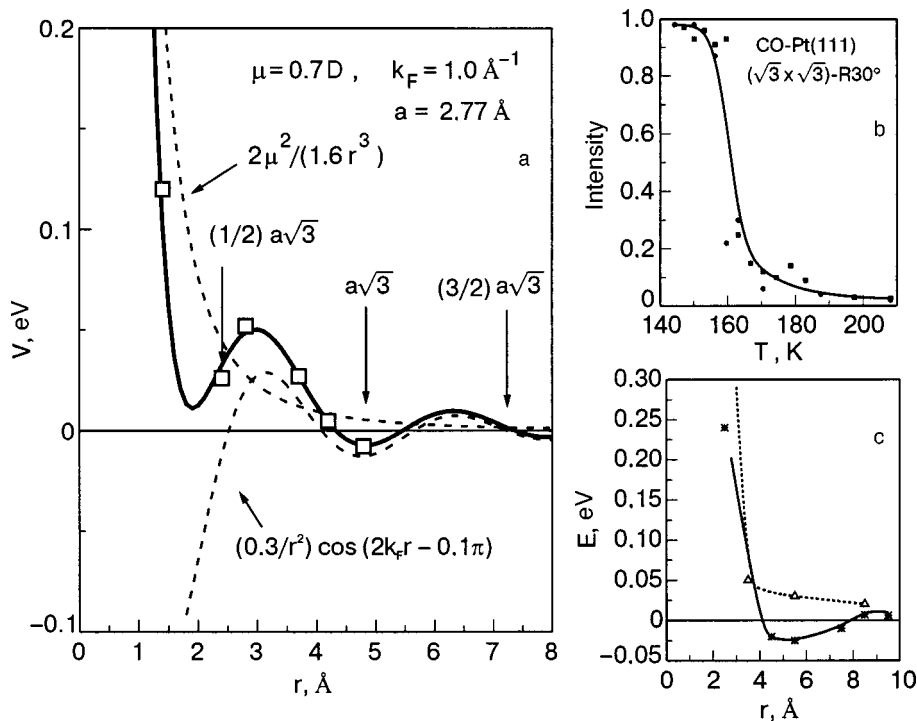


FIG. 11. Dependence of the model lateral interaction potential on the distance between CO molecules on the Pt(111) surface. The effective potential is constructed by adding together the dipole–dipole and an oscillatory indirect interaction. The symbols show the values of the interaction parameters obtained in the simulation (a). The temperature dependence of the intensity of a diffraction peak for the  $(\sqrt{3} \times \sqrt{3})R30^\circ$  structure<sup>56</sup> (b). The energies of the lateral interaction for CO on Pt(111), calculated in Ref. 63 (c).

initial decrease of the work function<sup>58</sup> turns out to be insufficient to account for the stability of the structure at 160 K, which is clearly seen in experiment. The disordering of the structure occurs at a temperature at which the energy  $kT$  of the fluctuations is of the order of the energy of the lateral interaction per particle. According to the results of the simulation, to obtain an order–disorder phase transition in the  $(\sqrt{3} \times \sqrt{3})R30^\circ$  structure at a temperature of 170 K it is necessary to postulate the presence of a dipole moment of around 2 D, which is much greater than the experimental value. This means that even at low coverages the interaction between adsorbed molecules has a more complex character. Since the  $(\sqrt{3} \times \sqrt{3})R30^\circ$  structure in CO films on Pt(111) is also observed<sup>59</sup> at  $\theta = 0.27$ , this is indicative of island growth of the structure, apparently due to the attraction between CO molecules at distances  $c = a\sqrt{3}$ . It is important to note that the distance  $c = a\sqrt{3}$ , corresponding to the lattice constants for the  $(\sqrt{3} \times \sqrt{3})R30^\circ$  structure, is preserved at the transition from one structure to another. Indeed, this same value is shared by the height of the triangle formed by molecules at the on-top centers in the  $(2 \times \sqrt{3})rect-2CO$  and  $c(5 \times \sqrt{3})rect-3CO$  structures, which correspond to coverages  $\theta = 0.5$  and  $\theta = 0.6$ . The presence of a quantity ( $c = a\sqrt{3}$ ) conserved in the structural transformations indicates that it is favorable for the molecules to lie at such a separation, i.e., it implies the existence of a local minimum of the lateral interaction potential.

The denser structures  $(2 \times \sqrt{3})rect-2CO$  and  $c(5 \times \sqrt{3})rect-3CO$ , which have lower symmetry than the surface, also inevitably presuppose the presence of a complex interaction that depends nonmonotonically on the distance between molecules.<sup>62–64,85–87</sup> At larger distances between molecules the effective attraction can come about only through indirect interaction<sup>89–91</sup> The indirect interaction potential oscillates with distance  $r$  between molecules, the pe-

riod of the oscillations being determined by the Fermi wave vector  $k_F$ :

$$V = Cr^{-n} \cos(2k_F r + \delta). \quad (3)$$

The asymptotics of the interaction is determined by the parameter  $n$ , which depends on the shape of the Fermi surface and the presence of bands of surface states crossing  $E_F$ . In the latter case  $n = 2$  and the indirect interaction is quite efficient.<sup>91,100</sup> Starting from the value of the modulus of the Fermi wave vector averaged over directions,  $k_F \approx 1 \text{ \AA}^{-1}$ , one can estimate the period of the Friedel oscillations as  $T = \pi/k_F \approx 3.1 \text{ \AA}$ . We assume further that the attraction between CO molecules at a distance of  $a\sqrt{3}$  is due to the minimum of the indirect interaction potential. This determines the choice of the initial phase, and for  $\delta = -0.1\pi$  the second minimum of the potential will be at a distance of  $a\sqrt{3}$  from a molecule located at the coordinate origin (Fig. 11). It should be emphasized that here the first minimum lies at a distance close to  $a\sqrt{3}/2$ , which agrees with the distance between nearest-neighbor molecules in the structures  $(2 \times \sqrt{3})rect-2CO$  and  $c(5 \times \sqrt{3})rect-3CO$  proposed for explaining the diffraction pattern at  $\theta = 0.5$  and  $\theta = 0.6$ , respectively (see Fig. 10). We also note that the distance to the center of the rectangular cell,  $3.66 \text{ \AA}$ , corresponds to a maximum of the indirect interaction potential, that can explain why the structure with the centered unit cell is energetically unfavorable and, consequently, does not form. Assuming that the lateral interaction between adsorbed CO molecules can be divided conventionally into a dipole–dipole (direct) and an indirect part, one can represent the result of their addition graphically as in Fig. 11a. The dipole–dipole repulsion between molecules smoothes out the first minimum of the potential somewhat at a distance  $a\sqrt{3}/2$ . This is apparently determined, in turn, by the absence of structures denser than  $(\sqrt{3} \times \sqrt{3})R30^\circ$  at  $\theta = 0.33$ . Thus the lateral interaction at  $\theta$

$=0.33$  in the model adopted here is described by dipole–dipole repulsion with energy  $2\mu/r^3$  (Ref. 90) and by the indirect interaction of the potential (3). For estimating the absolute values of the parameters of these interactions with the aid of a Monte Carlo simulation, one can use the data on the disordering of the  $(\sqrt{3}\times\sqrt{3})R30^\circ$  structure with increasing temperature. For example, at  $T=160$  K this structure is distinct and apparently well ordered,<sup>59</sup> while for  $T=170$  K the brightness of the reflections is somewhat lower,<sup>58</sup> indicating a partial disordering, and at  $T=300$  K this structure is essentially no longer visible for CO on Pt(111).<sup>58</sup> The values of the interaction parameters chosen for the simulations of the structure formation are shown by the symbols in Fig. 11a, and the calculated temperature dependence of the intensity of the diffraction peak for the  $(\sqrt{3}\times\sqrt{3})R30^\circ$  structure for those values is shown in Fig. 11b. As is seen in the figure, the values of the interaction parameters for different distances between CO molecules on Pt(111) are well described by the sum of the dipole–dipole and indirect interactions for  $\mu = 0.7$  D and  $C = 0.3$  eV·Å<sup>2</sup>.

As we have said, the sequence of filling of the adsorption centers with increasing CO coverage on Pt(111) attest to the advantage of the on-top centers. It is natural to assume that these centers are energetically more favorable than the bridge centers, because of the different energy of the adsorption bond for the CO molecules in these two types of centers. According to estimates made in Ref. 86 on the basis of quantum-mechanical calculations by the electron density functional method for different configurations of the clusters, the binding energy of a CO molecule with the Pt(111) surface in the on-top position is 1.64 eV, which is close to the experimental value 1.5 eV.<sup>60</sup> In the bridge position the binding energy is somewhat smaller, as is obvious from the fact that at low coverages the molecules occupy only on-top centers, and the difference in energy can be estimate only crudely as some hundredths of an electron-volt.<sup>58,63</sup> The presence of two types of adsorption centers on the surface permits one to use a modified lattice gas model in which the difference of the energies of the particles in sites of different types is taken into account (the energy benefit obtained when a CO molecule moves from a bridge to an on-top position was taken equal to 0.01 eV<sup>56</sup>).

Starting from the arguments adduced above, we chose for the simulation of the ordering of the adsorbed layer a matrix contains 72 rows and 120 columns for description of the two types of adsorption centers, which corresponds to a simulated piece of the Pt(111) surface approximately  $100 \times 100$  Å in size. This size of the simulated region approximates the coherence length of electrons for the standard LEED device and is therefore convenient for comparison of the simulated LEED patterns with the experimental ones, and it gives satisfactory statistics upon averaging over the particle distributions obtained after thermodynamic equilibrium is reached. It is assumed that the chosen part of the surface simulates an infinite Pt(111) surface, and so periodic boundary conditions were imposed.

The ordering procedure<sup>56,68–70,93,94</sup> is carried out as follows. First the particles were distributed randomly over adsorption centers, creating a specified coverage, and then, with a probability  $\exp(-\Delta E/k_B T)$ , a randomly chosen particle

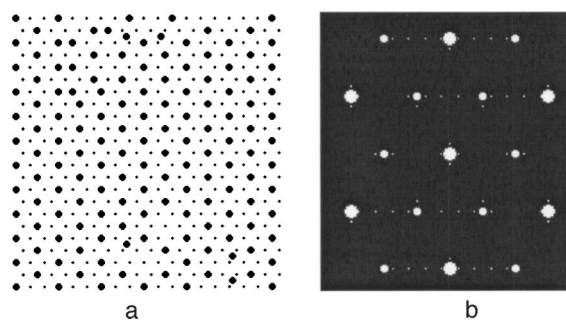


FIG. 12. Typical equilibrium distribution of particles on the model surface (a “snapshot”) obtained at  $\theta=0.33$  at a temperature below the disordering temperature<sup>56</sup> (a). The diffraction pattern calculated in the kinematic approximation agrees with the experimentally observed LEED pattern<sup>58</sup> at a temperature of 170 K (b).

is moved to a neighboring adsorption center. The energy difference is calculated with allowance for the lateral interaction and the difference of the adsorption energies at the two types of centers. If the move is energetically favorable ( $\Delta E < 0$ ) or is the probability  $\exp(-\Delta E/k_B T)$  is greater than a random number from the range (0–1), then the move is made. Otherwise the particle remains at the initial center. The number of moves made on average per particle is tallied. After 15–20 such moves, thermodynamic equilibrium is established in the system (corresponding to a minimum of the free energy; the total energy fluctuates about a minimum value that depends on temperature). If the temperature is below the temperature of the order–disorder transition, then domain structures corresponding to the chosen concentration are formed in the film, while at higher temperatures the film is disordered. Since the probability of a particle displacement is determined by the ratio  $\Delta E/k_B T$ , the values of the interaction parameters can be chosen so as to make the transition temperature match that observed in experiment (by the LEED method). Thus one can determine the numerical values of the parameters used in the simulation.

Figure 12 shows a typical equilibrium distribution of the particles over the model surface (a snapshot) at a coverage  $\theta=0.33$  and temperature 160 K, i.e., below the ordering temperature. The formation of a  $(\sqrt{3}\times\sqrt{3})R30^\circ$  domains structure with characteristic point defects (due to fluctuations) is clearly seen. The overwhelming majority of the particles occupy on-top adsorption centers, in agreement with the experimental data for CO on Pt(111). The diffraction pattern calculated in the kinematic approximation (according to formula (22)) is also in good agreement with the observed LEED pattern for this CO coverage at a temperature of 170 K.<sup>58</sup>

It is important to emphasize that the simulation of the  $(\sqrt{3}\times\sqrt{3})$  structure formation was done with the parameter values obtained from summing the dipole–dipole and indirect interaction potentials (see Fig. 11a). The parameter values shown by the symbols were also used in a simulation of the disordering of this structure (Fig. 11b) followed by the formation of denser structures at coverages of 0.5 and 0.6. The energies of the lateral interaction found in this way are in excellent agreement with the data of quantum-chemistry calculations from first principles<sup>63</sup> for the interaction energies between CO molecules at definite adsorption centers for

different distances between them (Fig. 11c). Here it should be noted that to explain the nonmonotonic<sup>62</sup> lateral interaction and the attraction between molecules at characteristic distances of 5–6 Å it is not necessary to invoke ternary interactions, as had previously been considered unavoidable.<sup>63</sup>

Apparently the ternary interactions become important in the formation of the  $(2 \times \sqrt{3})rect$ -2CO structure. As is seen in Fig. 11a, the first (local) minimum of the pair interaction potential can lead to the formation of the characteristic pairs of molecules for this structure, which lie at different adsorption centers a distance  $a\sqrt{3}/2$  apart. Clearly this position of the molecules, which probably coincides with the smallest possible distance between them, should lead to a redistribution of the electron density in the system. This may involve the partial depolarization of the dipoles and the corresponding changes in the parameters for the screening by substrate electrons. In this situation one would hardly expect that the indirect interaction potential created by a given pair on the surface would correspond to the sum of potentials formed by individual molecules.

In our study the ternary interaction was taken into account in the following way. In the direction along the pair of molecules the potential is assumed to be weakened (this was simulated by turning on an attraction due to the indirect pair interaction potential at a distance of  $a\sqrt{3}$ , and thus the interaction anisotropy arising in the formation of the  $(2 \times \sqrt{3})rect$ -2CO structure can be described in a natural way. As a result of the ordering of the film after approximately 30 displacements per particle, domains of this structure form, with a definite orientation of the lattice with respect to the Pt(111) surface (a small part of the simulated surface is shown in Fig. 13). It is probably the ternary interaction that leads to the formation of the domains of the  $(2 \times \sqrt{3})rect$ -2CO structure with the same definite arrangement of the molecules in the rectangular unit cells as is seen in the STM images<sup>78</sup> for such a structure of CO on Ni(111).

Indeed, in considering an individual unit cell it seems obvious that four similar structures with the same energy (and, hence, the same probability of formation) can be formed, namely, the given structure and the three structures obtained by reflection in the planes passing through the centers of the sides of the rectangular unit cell. The structures obtained by successive reflection in both planes (or by a 180° rotation about the center of the cell) are pairwise equivalent in the sense that they produce the same diffraction pattern (see Fig. 13), but the presence of other symmetric pairs of structures leads to a decrease of the intensity of certain reflections.

Thus the formation of domains of one orientation of the structure  $(2 \times \sqrt{3})rect$ -2CO requires the formation of initial nuclei of that orientation, “turning on” the ternary interactions. In the simulation such nuclei can be formed in a random manner (as was done in the case of the formation of the domains of the  $(2 \times \sqrt{3})rect$ -2CO structure), shown in Fig. 13) or can be specially introduced, imitating defects of a real surface. The diffraction pattern contains averaged information about a rather large part of the surface, with a size of the order of the electron beam diameter, within which several parts of area  $100 \times 100$  Å with different orientations of the

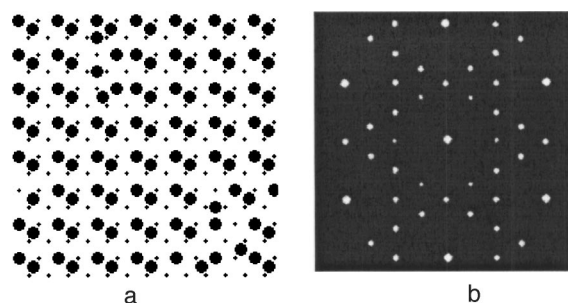


FIG. 13. Results of a simulation of the formation of the  $(2 \times \sqrt{3})rect$ -2CO structure: the equilibrium distribution of particles at a temperature of 300 K (a) and the diffraction pattern corresponding to it<sup>56</sup> (b).

domains of the  $(2 \times \sqrt{3})rect$ -2CO structure move about freely. Domains of this size are entirely sufficient to form a rather sharp diffraction pattern, which is obtained as a result of summing the contributions from structures with different orientations with respect to the three equivalent directions on the Pt(111) surface (Fig. 13).

#### 4.3. Kinetics of CO adsorption on Pt(111)

The most important disagreement between the results of the simulation of the CO oxidation reaction on the platinum surface with experiment remains the value of the limiting coverage ( $\theta=1$ ) obtained with the use of the ZGB algorithm<sup>68–72</sup> for CO adsorption in the absence of oxygen. Apparently the reason for this may be inadequate account of the lateral interaction between CO molecules and also the extremely simplified description of the surface as a lattice of adsorption centers of one type. Both of these shortcomings have been eliminated in a model proposed in Ref. 56, which holds forth the hope of a more correct description of the kinetics of CO adsorption on Pt(111).

A method of simulating the adsorption of gases in real time is described in detail in Ref. 45 and discussed above, and we shall therefore discuss only the details which are important for the kinetics of CO adsorption on Pt(111). At a fixed CO pressure the flux of particles to the surface is estimated by the Hertz–Knudsen formula and is expressed in fractions of a monolayer (i.e., the degree of coverage under the condition that the sticking coefficient  $S$  is equal to 1) per second. This allows one to express the exposure used in the simulation in langmuirs and to compare directly the adsorption isobars obtained with those observed in experiment.

The initial sticking coefficient of CO on Pt(111) was taken equal to 0.9 in accordance with experiment.<sup>101,102</sup> This is described in the simulation by an adsorption probability of 0.9 at a randomly chosen center on the clean surface (when the lateral interaction has not yet appeared, and all the centers are unoccupied). The role of extrinsic precursor states is also taken into account: a molecule striking the surface at an occupied center can be adsorbed at an unoccupied neighboring center.

After the adsorption has gone on for a certain time an ordering of the film occurs in the manner described in the previous Section, and then the desorption of molecules is simulated. Here it is assumed that the probability of desorption is determined by the Polanyi–Wigner equation with an

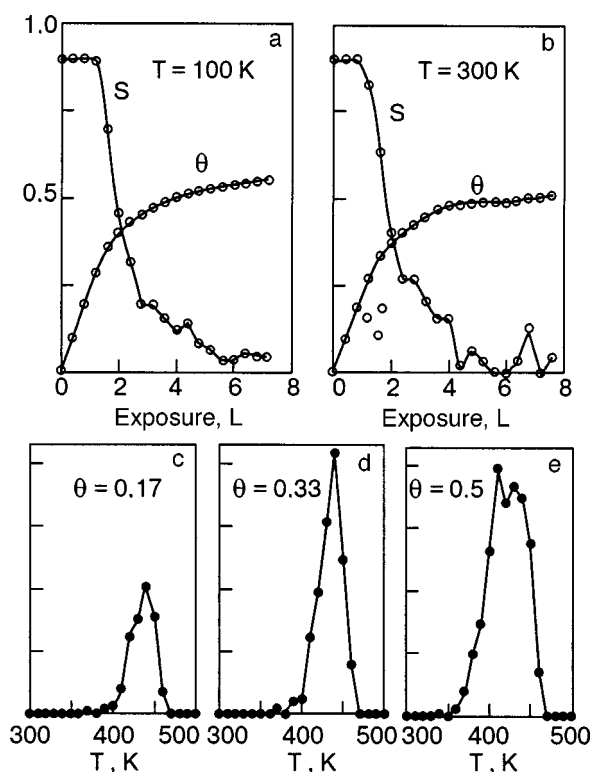


FIG. 14. Calculated dependence of the sticking coefficient  $S$  and degree of coverage  $\theta$  on the exposure (a,b), and the TPD spectra<sup>56</sup> for CO on Pt(111) obtained for different initial degrees of CO coverage (c,d,e).

activation energy that depends on the lateral interaction of the molecules.<sup>45,102</sup> In the description<sup>45</sup> of the kinetics of adsorption of molecular hydrogen on W(110) this algorithm demonstrated its ability to reproduce correctly both the dependence of the sticking coefficient on the coverage and the limiting coverages at different temperatures. The resulting dependence of the sticking coefficient  $S$  and coverage  $\theta$  on the exposure for CO on Pt(111) is shown in Fig. 14. As in experiment,<sup>58,60,101,102</sup> at low coverages the sticking coefficient is practically constant, attesting to the important role of extrinsic precursor states and the correctness of their description in the model used. As the coverage grows,  $S$  rapidly decreases, primarily because of the lateral interaction between adsorbed CO molecules and also the decrease of the number of unoccupied centers. As a result of the establishment of dynamic equilibrium, the CO coverage equals approximately 0.5, and for  $T = 300$  K it remains practically unchanged with time, while in the case of adsorption on a cooled surface ( $T = 100$  K) it continues to increase slowly, tending toward a value of around 0.6.

Using the standard Monte Carlo technique for simulating the temperature dependence of the desorption rate,<sup>45,55,96</sup> for the same kinetic parameters and interaction energies one can to good accuracy reproduce the spectrum observed<sup>60</sup> by temperature programmed desorption for CO on Pt(111) (Fig. 14). To facilitate comparison with experiment<sup>60</sup> the adsorption was simulated at  $T = 100$  K and was stopped after a specified coverage (0.17, 0.33, and 0.5) was reached, whereupon the substrate temperature was increased linearly at a rate of 15 K/s. At  $\theta = 0.17$ , when the lateral interaction as yet has practically no effect on the heat of adsorption, the maximum

on the TPD spectrum occurs at  $T = 480$  K. At larger coverages the lateral interaction, which is on average repulsive, becomes substantial and leads to a shift of the start of desorption to lower temperatures (Fig. 14), in good agreement with experiment.<sup>60</sup>

The temperature dependence of the limiting coverage obtained in the simulation is in good agreement with that observed experimentally for CO on Pt(111).<sup>58–60,101,102</sup> The kinetic parameters used in the simulation (desorption activation energy  $E_d = 1.2$  eV at a frequency factor  $\nu = 10^{13}$  s<sup>-1</sup>) also agree with those estimated in Refs. 58, 60–65, and 102.

## 5. STRUCTURE FORMATION AND ADSORPTION KINETICS OF OXYGEN ON Pt(111)

In the temperature range 25–150 K oxygen is adsorbed on the Pt(111) surface in molecular form, occupying adsorption sites with bridge type symmetry. The desorption peak of molecular oxygen is observed at 140–150 K, in agreement with the desorption activation energy  $\sim 0.36$ – $0.38$  eV.<sup>104</sup> Desorption of oxygen occurs from this molecular precursor state at a temperature above 150 K. First-principles calculations of the desorption energy with the use of the VASP code give a value of the barrier in the range 0.3 eV,<sup>105</sup> 0.38 eV,<sup>106</sup> 0.43 eV,<sup>107</sup> and, for different configurations of the position of the oxygen molecule relative to the Pt(111) surface, 0.3–1.5 eV.<sup>108</sup> Here atomic oxygen is adsorbed at adsorption sites with threefold symmetry and binds strongly with the surface. The TPD spectrum for oxygen displays two peaks: one corresponding to desorption from the molecule phase at a temperature of 140–150 K, and the other corresponding to dissociative desorption from the atomic state in the temperature region 600–1000 K.<sup>60,104,109</sup> Apparently the dissociation of the oxygen molecule near the metal surface is ultimately due to the occupation of the antibonding  $2\pi^*$  orbital.<sup>110,111</sup> On the hexagonal face of Pt(111) there are two types of adsorption centers of threefold symmetry, fcc and hcp, and the binding energy of atomic oxygen with the substrate is substantially different for the two types of sites. It is shown in Ref. 112 that the fcc centers are the stabler for the adsorption of oxygen, and the calculated activation energies of diffusion  $\text{fcc} \leftarrow \text{hcp}$  and  $\text{fcc} \rightarrow \text{hcp}$  are 0.13 and 0.58 eV, respectively.

The initial sticking coefficient for oxygen on Pt(111) is only 0.06.<sup>113–115</sup> One can alter the sticking coefficient substantially by the adsorption of active atoms and molecules that strongly affect the electron density distribution on the substrate surface. In the adsorption of alkali metals on Pt(111) their partial ionization leads to a redistribution of the electron density and creates local electric fields.<sup>111,116,117</sup> This results in a significant lowering of the potential barrier for chemisorption (the activation energy) and, in a number of cases, the probability of dissociative adsorption of oxygen can reach unity.<sup>118</sup>

It was shown in Refs. 119–124 that the presence of an electronegative adsorbate on the surface leads to a strong decrease in the rate of dissociative adsorption and in the limiting coverage and also to a significant change in the desorption parameters. The linear decrease of the initial sticking coefficient with increasing degree of coverage by an electronegative adsorbate attests to blocking of the mobile

precursor states for dissociative adsorption on the adsorbate-modified surface.<sup>113</sup>

Atomic oxygen on Pt(111) at temperatures in the range  $200\text{ K} < T < 350\text{ K}$  forms the ordered structure  $p(2 \times 2)$ , corresponding to a coverage of 0.25.<sup>59</sup> The limiting coverage achieved under different conditions of oxygen adsorption ranges from 0.22 to 0.28 ML.<sup>59,125</sup>

In order to obtain the correct value of the limiting coverage for system in a simulation one usually introduces parameters describing the desorption probability,<sup>69,72</sup> which makes it possible to avoid the complete poisoning of the model surface. It should be noted, however, that the oxygen desorption rate from the platinum surface at a temperature of the order of 400 K is negligible, and therefore the introduction of a desorption parameter can scarcely be justified physically; for this reason Sander and Ghaisas<sup>71</sup> have proposed (somewhat artificially) that oxygen requires three unoccupied neighboring sites for dissociative adsorption.

The results of a dynamic Monte Carlo simulation of the adsorption of molecular and atomic oxygen in the temperature range 100–200 K with dissociation, diffusion, and desorption taken into account are reported in Ref. 126. Also taken into account were the presence of a repulsive interaction up to third-nearest neighbors and the preference for adsorption of an oxygen atom at adsorption centers of fcc symmetry. A necessary condition for a molecular-oxygen desorption event is the presence of two unoccupied nearest adsorption centers of threefold symmetry. These conditions lead to a limitation of the possibility of adsorption at large coverages, and the limiting coverage obtained in such a model is 0.26, in good agreement with experiment. However, the experimentally observed  $p(2 \times 2)$  structure could not be obtained in the simulation, probably because of inadequate account of the lateral interaction in the model used.

It should be noted that the observed  $p(2 \times 2)$  structure is extremely rarefied, and for it to form at 300 K it is necessary to have a substantial interaction between adsorbed atoms. What sort of interaction can give rise to the formation of such structures? This lateral interaction might be dipole–dipole repulsion, although simple estimates show that if the formation of the  $p(2 \times 2)$  structure at room temperature were due solely to the dipole–dipole interaction, it would require a dipole moment of the oxygen adatom of 5 D, which is considerably larger than the value of the dipole moment of an oxygen atom on platinum estimated from the change of the work function.<sup>115</sup>

The indirect interaction between adatoms obviously plays an important role in the formation of oxygen structures on Pt(111). In the simulation, however, significant difficulties arise in the choice of initial parameters of the indirect interaction owing to the substantial variation of the electronic structure of the substrate with increasing oxygen concentration on the surface. This effect is due to the significant electronegativity of oxygen. For example, by means of self-consistent calculations of the electrostatic potential on the surface near an adsorbed electronegative atom in the jellium model, it was shown in Ref. 127 that the degree of poisoning of the surface increases with increasing electronegativity. The region in which the electrostatic potential acts is of the order of 3–4 Å, which corresponds to the distance to the

third- or fourth-nearest adsorption centers. Interestingly, the self-poisoning of the Pt(111) surface by oxygen does not prevent the adsorption of carbon monoxide, forming a  $c(2 \times 2)$  structure with the CO molecules located at the on-top center in the middle of the cell formed by oxygen adatoms.

The complexity of the interaction between adsorbed oxygen atoms on Pt(111) apparently is the reason why there are still no consistent and physically justified models for the formation of the observed structures. One expects that the solution of this pressing problem will open up new possibilities not only for deepening our understanding of the dissociative adsorption process for oxygen on a transition metal but will also broaden substantially the existing ideas as to the role of different factors in the kinetics of the catalytic reaction of CO oxidation.

## 6. CONCLUSION

The criteria of applicability and efficiency of a mathematical model include its ability to reproduce the main characteristics of the observed effects and also the degree to which it approximates the conditions of an experiment and the transparency of the results obtained. In this regard the Monte Carlo method of mathematical attempts is particularly well favored, since in many cases it not only makes it possible to explain many of the relationships observed in experiments but also to predict the behavior of the system under new conditions not yet investigated. It should be stressed that the simulation must always be based on firmly established facts, and its results must admit comparison with the data of real (or future) experiments—otherwise the simulation is of little value, since there are no other criteria for assessing the reliability of the results obtained and the conclusions drawn from them.

Examples of the efficient use of the Monte Carlo method for elucidating the properties of adsorption systems include the papers discussed in this review on the simulation of the low-temperature adsorption of hydrogen on W(110) and Mo(110), the adsorption and structure formation of CO films, and the catalytic reaction of CO oxidation on the platinum surface. For example, the model of molecular adsorption involving extrinsic precursor states has been validated and refined by simulations, and the activation energy for desorption of hydrogen molecules on the tungsten surface has been determined; this is important for the development of the theory of gas adsorption.

An important feature of the simulation methods described is the trend toward a detailed (to the degree possible) reproduction of the real conditions of an experiment and the incorporation of the most important factors governing the behavior of the system. This has made it possible to estimate the value and to elucidate the role of the lateral interaction in the establishment of thermodynamic equilibrium between the incident and desorbing fluxes of hydrogen molecules and also, with the aid of a real-time simulation algorithm developed, to propose an alternative explanation of the reason for the radical difference in the dynamics of oxygen adsorption on W(110) and Mo(110).

The use of a complex lattice of adsorption centers and the incorporation of the lateral interaction in the simulation of the formation of CO films on Pt(111) have made it pos-

sible not only to propose a novel (correct, i.e., in agreement with the experimentally observed sequence of diffraction patterns) arrangement of the molecules in the unit cell of the surface structures of CO on Pt(111), but also to obtain numerical values of the parameters of the indirect interaction that leads to the formation of those structures. By using the algorithm for the real-time simulation of the kinetic processes we have been able to obtain a correct value for the limiting CO coverage on Pt(111) and to reproduce the exposure dependence of the sticking coefficient.

The information obtained with the aid of simulations as to the structures of adsorbed CO films on Pt(111) and the parameters of the lateral interaction will obviously be useful for further studies of the catalytic reaction of CO oxidation and will open up new possibilities for a more detailed and realistic description of this reaction with the aid of refined simulation algorithms.

*Note added in proof:* Monte Carlo simulations using an advanced model for CO oxidation in Pt(111) have recently been carried out by N. V. Petrova and I. N. Yakovkin, Surf. Sci. **578**, 162 (2005).

\*E-mail: yakov@iop.kiev.ua

- <sup>1</sup>G. J. Kroes, Prog. Surf. Sci. **60**, 1 (1999).
- <sup>2</sup>A. Gross, Surf. Sci. **500**, 347 (2002).
- <sup>3</sup>S. Wilke and M. Scheffler, Phys. Rev. Lett. **B 53**, 4296 (1996).
- <sup>4</sup>A. Gross, M. Scheffler, M. J. Mehl, and D. A. Papaconstantopoulos, Phys. Rev. Lett. **82**, 1209 (1999).
- <sup>5</sup>A. Gross and M. Scheffler, Phys. Rev. Lett. **B 57**, 1293 (1999).
- <sup>6</sup>G. Wiesenecker, G. J. Kroes, and E. J. Baerends, J. Chem. Phys. **104**, 7344 (1996).
- <sup>7</sup>C. M. Wei, A. Gross, and M. Scheffler, Phys. Rev. Lett. **B 57**, 15572 (1998).
- <sup>8</sup>J. A. White, D. M. Bird, and M. C. Payne, Phys. Rev. Lett. **B 53**, 1667 (1996).
- <sup>9</sup>W. Kohn, Surf. Rev. Lett. **1**, 129 (1994).
- <sup>10</sup>H. J. Kreuzer, S. H. Payne, A. Drozdowski, and D. Menzel, J. Chem. Phys. **110**, 6982 (1999).
- <sup>11</sup>G. R. Darling and S. Holloway, Surf. Sci. **321**, L189 (1994).
- <sup>12</sup>S. Holloway and G. R. Darling, Surf. Rev. Lett. **1**, 115 (1994).
- <sup>13</sup>M. Persson and S. Andersson, Surf. Rev. Lett. **1**, 187 (1994).
- <sup>14</sup>M. Bonn, A. W. Kleyn, and G. J. Kroes, Surf. Sci. **500**, 475 (2002).
- <sup>15</sup>E. Hulpke and J. Ludecke, Phys. Rev. Lett. **68**, 2846 (1992).
- <sup>16</sup>B. Kohler, P. Ruggerone, and M. Scheffler, Surf. Sci. **368**, 213 (1996).
- <sup>17</sup>B. Kohler, P. Ruggerone, and M. Scheffler, Phys. Rev. Lett. **B 56**, 13503 (1997).
- <sup>18</sup>Yu. G. Ptushinskii, Fiz. Nizk. Temp. **30**, 3 (2004) [Low Temp. Phys. **30**, 1 (2004)].
- <sup>19</sup>V. V. Dvurechenskikh, V. D. Osovskii, Yu. G. Ptushinskii, V. G. Sukretnyi, and B. A. Chuikov, JETP Lett. **54**, 40 (1991).
- <sup>20</sup>J. Harris and S. Andersson, Phys. Rev. Lett. **B 55**, 1583 (1985); S. Andersson, L. Wilzen, M. Persson, and J. Harris, *ibid.* **40**, 8146 (1989).
- <sup>21</sup>W. Friess, H. Schlichting, and D. Menzel, Phys. Rev. Lett. **74**, 1147 (1995).
- <sup>22</sup>K. D. Rendulic, G. Anger, and A. Winkler, Surf. Sci. **208**, 404 (1989).
- <sup>23</sup>H. F. Berger, C. Resch, E. Grosslinger, G. Eilmsteiner, A. Winkler, and K. D. Rendulic, Surf. Sci. **275**, L627 (1992).
- <sup>24</sup>D. A. Butler, B. E. Hayden, and J. D. Jones, Chem. Phys. Lett. **217**, 423 (1994).
- <sup>25</sup>D. A. Butler and B. E. Hayden, Chem. Phys. Lett. **232**, 542 (1995).
- <sup>26</sup>V. D. Osovskii, Yu. G. Ptushinskii, V. G. Sukretnyi, and B. A. Chuikov, JETP Lett. **67**, 959 (1998).
- <sup>27</sup>B. A. Chuikov, V. D. Osovskii, Yu. G. Ptushinskii, and V. G. Sukretnyi, Surf. Sci. Lett. **448**, L201 (2000).
- <sup>28</sup>B. A. Chuikov, V. D. Osovskii, Yu. G. Ptushinskii, and V. G. Sukretnyi, Surf. Sci. **473**, 143 (2001).
- <sup>29</sup>M. Beutl, J. Lesnik, and D. K. Rendulic, Surf. Sci. **429**, 71 (1999).
- <sup>30</sup>Ch. Resch, H. F. Berger, K. D. Rendulic, and E. Bertel, Surf. Sci. **316**, L1105 (1994).
- <sup>31</sup>D. A. Papaconstantopoulos, *Handbook of the Band Structure of Elemental Solids*, Plenum Press, New York (1986).
- <sup>32</sup>Y. Xu and I. I. Fabrikant, Appl. Phys. Lett. **78**, 2598 (2001).
- <sup>33</sup>T. O. O'Malley, Phys. Rev. Lett. **B 150**, 150 (1966).
- <sup>34</sup>P. W. Tamm and L. D. Schmidt, J. Chem. Phys. **54**, 4775 (1971).
- <sup>35</sup>K. Christmann, Surf. Sci. Rep. **9**, 1 (1988).
- <sup>36</sup>P. Alnot, A. Cassuto, and D. A. King, Surf. Sci. **215**, 29 (1989).
- <sup>37</sup>K. D. Rendulic, Surf. Sci. **272**, 34 (1992).
- <sup>38</sup>A. Gross, S. Wilke, and M. Scheffler, Phys. Rev. Lett. **75**, 2718 (1995).
- <sup>39</sup>M. Kay, G. R. Darling, S. Holloway, J. A. White, and D. M. Bird, Chem. Phys. Lett. **245**, 311 (1995).
- <sup>40</sup>H. F. Busnengo, W. Dong, and A. Salin, Chem. Phys. Lett. **320**, 328 (2000).
- <sup>41</sup>M. A. Di Cesare, H. F. Busnengo, W. Dong, and A. Salin, J. Chem. Phys. **118**, 11226 (2003).
- <sup>42</sup>M. R. Hand and J. Harris, J. Chem. Phys. **92**, 7610 (1990).
- <sup>43</sup>H. Schlichting and D. Menzel, Surf. Sci. **272**, 27 (1992).
- <sup>44</sup>A. Gross, Surf. Sci. **363**, 1 (1996).
- <sup>45</sup>N. V. Petrova, I. N. Yakovkin, and Yu. G. Ptushinskii, Surf. Sci. **497**, 349 (2002).
- <sup>46</sup>Yu. G. Ptushinskii and B. A. Chuikov, Poverkhnost' **9**, 5 (1992).
- <sup>47</sup>N. V. Petrova, I. N. Yakovkin, and Yu. G. Ptushinskii, Eur. Phys. J. B **38**, 525 (2004).
- <sup>48</sup>V. D. Osovskii, Yu. G. Ptushinskii, V. G. Sukretnyi, and B. A. Chuikov, JETP Lett. **60**, 569 (1994).
- <sup>49</sup>V. D. Osovskii, Yu. G. Ptushinskii, V. G. Sukretnyi, and B. A. Chuikov, Low Temp. Phys. **23**, 587 (1997).
- <sup>50</sup>H. Schlichting, D. Menzel, T. Brunner, and W. Brenig, J. Chem. Phys. **97**, 4453 (1992).
- <sup>51</sup>M. Head-Gordon, J. C. Tully, H. Schlichting, and D. Menzel, J. Chem. Phys. **95**, 9266 (1991).
- <sup>52</sup>V. D. Osovskii, Yu. G. Ptushinskii, V. G. Sukretnyi, and B. A. Chuikov, Fiz. Nizk. Temp. **27**, 1138 (2001) [Low Temp. Phys. **27**, 843 (2001)].
- <sup>53</sup>C. M. Chan, R. Aris, and W. H. Weinberg, Appl. Surf. Sci. **1**, 360 (1978).
- <sup>54</sup>J. L. Taylor and W. H. Weinberg, Surf. Sci. **78**, 259 (1978).
- <sup>55</sup>B. Meng and W. Y. Weinberg, J. Chem. Phys. **100**, 5280 (1994).
- <sup>56</sup>N. V. Petrova and I. N. Yakovkin, Surf. Sci. **519**, 90 (2002).
- <sup>57</sup>R. Imbühl, Prog. Surf. Sci. **44**, 185 (1993).
- <sup>58</sup>G. Ertl, M. Neumann, and K. M. Streit, Surf. Sci. **64**, 393 (1977).
- <sup>59</sup>P. R. Norton, J. A. Davies, and T. E. Jackman, Surf. Sci. Lett. **122**, L593 (1982).
- <sup>60</sup>H. Steininger, S. Lehwald, and H. Ibach, Surf. Sci. **123**, 264 (1982).
- <sup>61</sup>B. N. J. Persson and R. Ryberg, Phys. Rev. Lett. **40**, 20173 (1989).
- <sup>62</sup>D. C. Skelton, D. H. Wei, and S. D. Kevan, Surf. Sci. **320**, 77 (1994).
- <sup>63</sup>D. R. Jennison, P. A. Schultz, and M. P. Sears, Phys. Rev. Lett. **77**, 4828 (1996).
- <sup>64</sup>R. Brako and D. Sokcevic, Surf. Sci. **401**, L388 (1998).
- <sup>65</sup>K. L. Kostov, P. Jakob, and D. Menzel, Surf. Sci. **377–379**, 802 (1997).
- <sup>66</sup>F. Debecq, Surf. Sci. **389**, L1131 (1997).
- <sup>67</sup>I. N. Yakovkin, V. I. Chernyi, and A. G. Naumovets, Surf. Sci. **442**, 81 (1999).
- <sup>68</sup>R. M. Ziff, E. Gulary, and Y. Barshad, Phys. Rev. Lett. **24**, 2553 (1986).
- <sup>69</sup>J. Mai, W. von Niessen, and A. Blumen, J. Chem. Phys. **93**, 3685 (1990).
- <sup>70</sup>R. Chakarova, Surf. Sci. **389**, 234 (1997).
- <sup>71</sup>L. M. Sander and S. V. Ghaisas, Surf. Sci. **391**, 125 (1997).
- <sup>72</sup>M. Ehsani, M. Matloch, O. Frank, J. H. Block, K. Christmann, F. S. Rys, and W. Hirschwald, J. Chem. Phys. **91**, 4949 (1989).
- <sup>73</sup>V. K. Medvedev, Yu. Suchorski, and J. H. Block, Appl. Surf. Sci. **76/77**, 136 (1994).
- <sup>74</sup>P. Hollins and J. Pritchard, Surf. Sci. **99**, L389 (1980).
- <sup>75</sup>K. Christmann, O. Schober, and G. Ertl, J. Chem. Phys. **60**, 4719 (1974).
- <sup>76</sup>H. Conrad, G. Ertl, J. Kupperts, and E. E. Latta, Surf. Sci. **57**, 475 (1976).
- <sup>77</sup>L. Becker, S. Aminpirooz, B. Hillert, M. Pedio, J. Haase, and D. L. Adams, Phys. Rev. Lett. **B 47**, 9710 (1993).
- <sup>78</sup>Norihito Ikemiyama, Toshiaki Suzuki, and Masatoshi Ito, Surf. Sci. **466**, 119 (2000).
- <sup>79</sup>R. Davis, R. Toomes, D. P. Woodruff, O. Schaff, V. Fernández, K.-M. Schindler, Ph. Hofmann, K.-U. Weiss, R. Dippel, V. Fritzsche, and A. M. Bradshaw, Surf. Sci. **393**, 12 (1997).
- <sup>80</sup>L. D. Mapledoram, M. P. Bessent, A. Wander, and D. A. King, Chem. Phys. Lett. **228**, 527 (1994).
- <sup>81</sup>L. Surnev, Z. Xu, and J. T. Yates, Jr., Surf. Sci. **201**, 1 (1988).
- <sup>82</sup>M. Gieré, A. Barbieri, M. A. Van Hove, and G. A. Somorjai, Surf. Sci. **391**, 176 (1997).

- <sup>83</sup>D. H. Wei, D. C. Skelton, and S. D. Kevan, *Surf. Sci.* **381**, 49 (1997).
- <sup>84</sup>B. Reidmuller, I. M. Ciobica, D. C. Papageorgopoulos, B. Berenbak, R. A. van Santen, and A. W. Kleyn, *Surf. Sci.* **465**, 347 (2000).
- <sup>85</sup>J. J. Mortensen, B. Hammer, and J. K. Norskov, *Surf. Sci.* **414**, 315 (1998).
- <sup>86</sup>Y. Morikawa, J. J. Mortensen, B. Hammer, and J. K. Norskov, *Surf. Sci.* **386**, 67 (1997).
- <sup>87</sup>Hideaki Aizawa and Shinji Tsuneyuki, *Surf. Sci.* **399**, L364 (1998).
- <sup>88</sup>N. Pavlenko, P. P. Kostrobij, Yu. Suchorski, and R. Imbihl, *Surf. Sci.* **489**, 29 (2001).
- <sup>89</sup>T. B. Grimley, *Proc. Phys. Soc. London* **90**, 751 (1967).
- <sup>90</sup>T. L. Einstein, *CRC Crit. Rev. Sol. St. and Mat. Sci.* **7**, 261 (1978).
- <sup>91</sup>O. M. Braun and V. K. Medvedev, *Sov. Phys. Usp.* **32**, 328 (1989).
- <sup>92</sup>T. T. Tsong, *Surf. Sci.* **122**, 99 (1982).
- <sup>93</sup>J. Koppers, *Vacuum* **21**, 393 (1971).
- <sup>94</sup>I. N. Yakovkin, *Surf. Sci.* **282**, 195 (1993).
- <sup>95</sup>I. Hasegawa and S. Ino, *Phys. Rev. Lett.* **68**, 1192 (1992).
- <sup>96</sup>B. Lehner, M. Hohage, and P. Zeppenfeld, *Surf. Sci.* **454–456**, 251 (2000).
- <sup>97</sup>K. Fichthorn, E. Gulari, and R. Ziff, *Surf. Sci.* **243**, 273 (1991).
- <sup>98</sup>L. D. Roelofs, R. L. Park, and T. L. Einstein, *J. Vac. Sci. Technol.* **16**, 478 (1979).
- <sup>99</sup>V. K. Medvedev and I. N. Yakovkin, *Sov. Phys. Solid State* **19**, 1515 (1977).
- <sup>100</sup>O. M. Braun, L. G. Ilchenko, and E. A. Pashitsky, *Sov. Phys. Solid State* **22**, 1649 (1980).
- <sup>101</sup>I. N. Yakovkin, V. I. Chernyi, and A. G. Naumovets, *J. Phys. D: Appl. Phys.* **32**, 841 (1999).
- <sup>102</sup>M. Kiskinova, G. Pirug, and H. P. Bonzel, *Surf. Sci.* **133**, 321 (1983).
- <sup>103</sup>C. Puglia, A. Nilsson, B. Hernnas, O. Karis, P. Bennich, and N. Martensson, *Surf. Sci.* **342**, 119 (1995).
- <sup>104</sup>A. Winkler, X. Guo, H. R. Siddiqui, P. L. Hagans, and J. T. Yates, *Surf. Sci.* **201**, 419 (1988).
- <sup>105</sup>T. Li and P. B. Balbuena, *J. Phys. Chem. B* **105**, 9943 (2001).
- <sup>106</sup>J. L. Gland, *Surf. Sci.* **93**, 487 (1980).
- <sup>107</sup>C. T. Campbell, G. Ertl, H. Kuipers, and Segner, *J. Surf. Sci.* **107**, 220 (1981).
- <sup>108</sup>A. Eichler and J. Hafner, *Phys. Rev. Lett.* **79**, 4481 (1997).
- <sup>109</sup>X.-Y. Zhu, S. R. Hatch, A. Campion, and J. M. White, *J. Chem. Phys.* **91**, 5011 (1989).
- <sup>110</sup>A. Zangwill, *Physics at Surfaces*, Cambridge Univ. Press, Cambridge (1986), Mir, Moscow (1990).
- <sup>111</sup>M. Kiskinova, *Studies in Surface Science and Catalysis*, Elsevier (1992), Vol. 70, p. 1.
- <sup>112</sup>A. Bogicevic, J. Stromquist, and B. I. Lundqvist, *Phys. Rev. Lett.* **B57**, R4289 (1998).
- <sup>113</sup>M. P. Kiskinova, *Surf. Sci. Rep.* **8**, 359 (1988).
- <sup>114</sup>L. Surnev, *Physics and Chemistry of Alkali Metal Adsorption*, Elsevier (1989).
- <sup>115</sup>G. Pirug, H. P. Bonzel, and G. Broden, *Surf. Sci.* **122**, 1 (1982).
- <sup>116</sup>J. K. Brown and N. Lunz, *Chem. Phys. Lett.* **186**, 125 (1991).
- <sup>117</sup>J. Norskov, S. Holloway, and N. D. Lang, *Surf. Sci.* **137**, 65 (1984).
- <sup>118</sup>H. P. Bonzel, *Surf. Sci. Rep.* **84**, 3 (1988).
- <sup>119</sup>M. Kiskinova and D. W. Goodman, *Surf. Sci.* **109**, L555 (1981).
- <sup>120</sup>M. Kiskinova and D. W. Goodman, *Surf. Sci.* **108**, 64 (1981).
- <sup>121</sup>D. W. Goodman and M. Kiskinova, *Surf. Sci.* **105**, L256 (1981).
- <sup>122</sup>S. Johnson and R. J. Madix, *Surf. Sci.* **108**, 77 (1981).
- <sup>123</sup>E. I. Ko and R. J. Madix, *Surf. Sci.* **109**, 221 (1981).
- <sup>124</sup>K. D. Rendulic and A. Winkler, *Surf. Sci.* **74**, 318 (1978).
- <sup>125</sup>A. Szabo, M. Kiskinova, and J. T. Yates, Jr., *J. Chem. Phys.* **90**, 4604 (1989).
- <sup>126</sup>D. S. Mainardi, S. R. Calvo, A. P. J. Jansen, J. J. Lukkien, and P. B. Balbuena, *Chem. Phys. Lett.* **382**, 553 (2003).
- <sup>127</sup>N. D. Lang, S. Holloway, and J. K. Norskov, *Surf. Sci.* **150**, 24 (1985).

Translated by Steve Torstveit